Published in final edited form as:
J Oral Maxillofac Surg. 2015 March ; 73(3): 451–464. doi:10.1016/j.joms.2014.09.019.

Microbial biofilms are able to destroy hydroxyapatite in the absence of host immunity *in vitro*

Adam Feliks Junka, PhD[1,*], **Patrycja Szymczyk, MEng**[2], **Danuta Smutnicka, MS**[1], **Marcin Kos, MD, DDS, PhD**[3], **Iryna Smolina, MEng**[2], **Marzenna Bartoszewicz, AP**[1], **Edward Chlebus, Prof**[2], **Michal Turniak, MEng**[1], and **Parish P. Sedghizadeh, DDS, MS**[4]

[1] Department of Pharmaceutical Microbiology and Parasitology, Medical University of Wroclaw, Borowska 211a Street, 50-556 Wrocław [2] Centre for Advanced Manufacturing Technologies, Wroclaw University of Technology, Lukasiewicza Street. 5, 50-371 Wroclaw, Poland [3] Department of Maxillofacial and Plastic Surgery, Klinikum Oldenburg, Oldenburg, Germany [4] USC Ostrow School of Dentistry, USC Center for Biofilms, 925 West 34th Street #4110, Los Angeles, CA 90089-0641, USA

Abstract

Introduction—It is widely thought that inflammation and osteoclastogenesis result in hydroxyapatite (HA) resorption and sequestra formation during osseous infections, and microbial biofilm pathogens induce the inflammatory destruction of HA. We hypothesized that biofilms associated with infectious bone disease can directly resorb HA in the absence of host inflammation or osteoclastogenesis. Therefore, we developed an *in vitro* model to test this hypothesis.

Materials and Methods—Customized HA discs were manufactured as a substrate for growing clinically relevant biofilm pathogens. Single-species biofilms of *S.mutans, S.aureus, P.aeruginosa and C.albicans*, and mixed-species biofilms of *C.albicans* + *S.mutans* were incubated on HA discs for 72 hours to grow mature biofilms. Three different non-biofilm control groups were also established for testing. HA discs were then evaluated by means of scanning electron microscopy, micro-CT metrotomography, x-ray spectroscopy and confocal microscopy with planimetric analysis. Additionally, quantitative cultures and pH assessment were performed. ANOVA was used to test for significance between treatment and control groups.

Results—All investigated biofilms were able to cause significant ($P<0.05$) and morphologically characteristic alterations in HA structure as compared to controls. The highest number of alterations observed was caused by mixed biofilms of *C.albicans* + *S.mutans.* S. mutans biofilm

[*]**Corresponding author:** Adam Feliks Junka Department of Pharmaceutical Microbiology and Parasitology, Medical University of Wroclaw, Borowska 211a Street, 50-556 Wrocław tel. [071]7841301, feliks.junka@gmail.com.

incubated in medium with additional sucrose content was the most detrimental to HA surfaces among single-species biofilms.

Conclusion—These findings suggest that direct microbial resorption of bone is possible in addition to immune-mediated destruction, which has important translational implications for the pathogenesis of chronic bone infections and for targeted antimicrobial therapeutics.

Keywords

biofilm; hydroxyapatite; bone; sequestra; osteomyelitis; osteonecrosis

1. INTRODUCTION

Most osseous infections are caused by microbial biofilms, a concept elucidated only in recent decades owing to advancements in modern microbiology detection and imaging techniques.[1] Biofilms are characterized by a complex community of microbial cells that are attached to a surface and are embedded in a matrix of extracellular polymeric substance. Biofilm organisms exhibit an altered phenotype with respect to growth rate, gene transcription, and antimicrobial resistance as compared with their planktonic or free-floating counterparts.[2] Therefore, accurate diagnosis or treatment of chronic biofilm-mediated bone infections can be clinically challenging.

Persistent bone infections such as chronic osteomyelitis, jaw osteonecrosis, or periodontitis can all culminate in significant destruction of hydroxyapatite (HA).[3,4,5] Although HA resorption is thought to be induced and mediated by microbial biofilm pathogens, it is considered predominantly the result of inflammatory and osteoclastogenic activity.[6,7] Various inflammatory cells and cytokines can contribute to bone necrosis or HA resorption in these diseases. In chronic osteomyelitis and in jaw osteonecrosis, for example, vascular channels can become compressed and obliterated by the inflammatory process, and the resulting ischaemia further contributes to bone necrosis. Segments of non-vital bone devoid of blood supply can become separated to form *sequestra* which can continue to harbour microbes despite antibiotic treatment; antibiotics and inflammatory cells cannot reach avascular sequestra, so conservative medical treatment fails.[1,4]

A hallmark of chronic osteomyelitis and jaw osteonecrosis is sequestra formation that is evident radiographically, histopathologically, and clinically or surgically. The recent emergence of chronic jaw osteomyelitis or osteonecrosis associated with antiresorptive therapy has provided interesting insights into sequestra formation clinically. Because this jawbone disease is chronic and indolent, and defined by the presence of sequestra visible in the oral cavity for more than 8 weeks,[8] and because it is difficult to resolve with no known cure, it is not unusual for clinicians to observe the open jawbone wound and infection for months to years without resolution despite antibiotic therapy or surgical intervention. From clinical observations in this setting we have noticed sequestra formation that continues to resorb or change over time in the absence of inflammation given the avascular nature of the lesion. Bone biopsy specimens from this condition demonstrate histopathologic evidence of bone resorption and osteocyte dropout from lacunae in regions where no eukaryotic cells are present, such as leukocytes or osteoclasts, within or adjacent to resorption pits.[9]

Furthermore, given that patients with this form of jaw osteomyelitis receive antiresorptive medications to prevent osteoclastogenesis, and sometimes concomitant with steroids which suppress immunity, the degree of bone resorption seen is unlikely until we consider the possibility of direct resorption by bacteria.

Based on clinico-pathologic and surgical observations in chronic bone infections, combined with recent findings from advanced imaging studies and high-powered microscopic techniques into biofilm evaluation of bone infections,[10,11] we suggest that biofilms associated with bone infections can directly resorb or destroy HA in the absence of host inflammation or osteoclastogenesis. It is possible that direct biofilm-mediated bone resorption (in addition to inflammatory-mediated resorption) plays a role in the pathogenesis of chronic bone infections such as osteomyelitis, osteonecrosis, or periodontitis. The literature is replete with *in vivo* or animal models of chronic bone infections showing that HA destruction is secondary to inflammation, which is induced and modulated by biofilm pathogens. Our goal was to intentionally perform an *in vitro* study rather than *in vivo* in order to preclude a host immune response or inflammatory mediators, so that we may observe solely the qualitative and quantitative effects of microbial biofilms on HA surfaces.

We hypothesize that pathogens associated with common chronic infectious diseases of bone have the ability to resorb or alter bone in the absence of host immunity. As proof of this principle, we designed and conducted several experiments.

2. MATERIALS AND METHODS

Experimental strains

For experimental purposes, the following American Type Culture Collection (ATCC) strains were used: *Staphylococcus aureus* 6538, *Pseudomonas aeruginosa* 15442, *Streptococcus mutans* 25175, and *Candida albicans* 10231. For the experiments as described in the section to follow entitled: “Frequency of occurrence of specific pseudomonal-induced alterations”, twenty clinical strains isolated from different orthopaedic infections (part of the strains collection of the Wroclaw Microbiology Department), were used. The rationale for using these specific organisms in our study is predicated on the high prevalence of these organisms in association with common bone infections, providing for translational potential and clinical insight into infectious bone disease etiopathogenesis. *S.aureus* is by far the most common cause of long bone osteomyelitis; *P.aeruginosa* can be seen in vertebral osteomyelitis in patients with urinary catheters in place for long periods; *C.albicans* is commonly seen in jaw osteonecrosis in co-aggregation with bacteria like streptococci, and is also seen in fungal osteomyelitis as a complication of catheter-related fungemia; *S.mutans* is a common oral pathogen identified in cases of jaw osteonecrosis, periodontitis and caries.

Manufacture of HA Discs

Commercially available HA powder MT3300 (LOW-WET, Tomita Pharmaceutical Co., Ltd. Japan) was used for custom disc manufacturing. This particular HA powder is of heterogeneous spherical shape and of 50-200μm particle size. Powder pellets of 9.6mm diameter were pressed without a binder. Sinter was performed at 900 °C. The tablets were

compressed using the Universal Testing System for Static Tensile, Compression and Bending Tests, INSTRON 3384. The quality of the manufactured HA discs was checked by means of confocal microscopy and micro-computed tomography (CT), using a LEXT OLS4000 microscope (Olympus) and Metrotom 1500 microtomograph (Carl Zeiss), respectively. Micro-CT metrotomography was applied for analysing and measuring the internal and external geometries of manufactured HA discs. Micro-CT data was analysed using VG Studio MAX software (Volume Graphics GmbH, Heidelberg, Germany).

Confirmation of tested strains ability to form biofilm on HA discs

Strain incubation and sample preparation for scanning electron microscopy

Strains, cultured on agar plates, were transferred to tryptic soy broth (TSB) medium and incubated at 37°C for 24 hrs in aerobic conditions. The exception was *S.mutans*, which was transferred to brain-heart infusion medium (BHIM) supplemented with 3% sucrose (BHIM +3%S) and incubated in facultative anaerobic conditions. During the course of experimentation, it was also necessary to incubate *S.mutans* in BHIM without sucrose to limit its ability to form plaque (all other conditions similar). After incubation, the densities of the microbial suspensions were measured using a densitometer (Biomerieux Poland; Warsaw, Poland) and diluted to the density of 1 McFarland (MF). The microbial dilutions were incubated with HA discs at 37°C for 72 hrs. To obtain a mixed biofilm, 1mL of 1MF *Str.mutans* and 1MF of *C.albicans* were mixed and then transferred to the HA disc-containing wells. After incubation, discs were rinsed using physiologic saline to remove non-adherent organisms and to leave only biofilm-forming species. Subsequently, the discs were fixed using 3% glutarate (Poch, Gliwice, Poland) for 15 minutes at room temperature. Then, the samples were rinsed twice with phosphate buffer (Sigma Aldrich Poland; Poznan, Poland) to remove the fixative. The next step was dehydration in increasing concentrations of ethanol (25%, 50%, 60%, 70%, 80%, 90%, and 100%) for 10 minutes in each solution. After rinsing off the ethanol, the samples were dried at room temperature. Then, the samples were covered with gold and palladium (60:40; sputter current, 40 mA; sputter time, 50 seconds) using a Quorum machine (Quorum International; Fort Worth, TX) and examined under a Zeiss EVO MA25 scanning electron microscope (SEM). Strains were considered competent to form biofilm if they were able to adhere to the HA surface and if they were, at least partially, embedded within extracellular biofilm matrix.

Quantitative cultures

Microbial dilutions were incubated with HA discs at 37°C for 72 hrs as described in the above section. After incubation, the discs were rinsed using physiologic saline and transferred to 1 mL of 0.5% saponine (Sigma-Aldrich). HA discs were vortex-mixed vigorously for 1 minute to detach cells from the HA surface. After vortex mixing, the microbial suspensions were diluted 10 to 10^7 times. Each dilution (100 μL) was cultured on the appropriate stable medium and incubated at 37°C for 24 hrs. After this time, the microbial colonies were counted and the number of cells forming biofilm was assessed. All measurements were repeated 3 times. Results were presented as the mean number of colony forming units (cfu) per square millimetre of HA disc surface ± standard error of the mean.

To estimate the exact surface area of each HA disc, x-ray tomographic analysis was applied in a manner detailed by us previously.[12]

Ability of tested strains to cause alterations on HA surfaces

Strain incubation and biofilm removal

Each strain's 1MF suspension was divided into 6 aliquots of 2mL. Each aliquot was transferred to the well of a 24-well plate (CellStar, Germany). Each well contained one HA disc. Strains were allowed to from biofilm on HA discs in the conditions specified in **Table 1.** After 72 hrs, discs with biofilm on it were gently rinsed using physiologic saline to remove non-adherent bacteria. Rinsed discs were transferred to new 24-well plates filled with 2mL of 10% saponine detergent (Sigma Aldrich, Poland), and left for 20 minutes at room temperature. After incubation, plates were mounted into a plate shaker (Schnuttler MTS 2, Ika) for 2 minutes at speed 1000/min. This led to mechanical removal of biofilm from the HA disc surface. After shaking, discs were rinsed with ultrapure water and dried at room temperature. Again, *S.mutans* biofilm incubated in BHIM+3% sucrose medium formed plaque structures resistant to that type of treatment. Therefore, plaque was subjected to 20 minutes of incubation with 10% saponine, and then it was gently removed with a woollen swab. Subsequently, discs with partially removed plaque were subjected to shaking for 2 minutes at speed 1000/min.

Preparation of cell-free supernatant

After 72 hrs of biofilm incubation, medium was taken from the wells. Since it contained planktonic cells, it was filtered through 0.20μm filters (Sarstedt, Warsaw) to obtain a cell-free supernatant. It was then introduced to a well containing a new sterile HA disc, and left for another 72 hrs. Next, the supernatant was removed; HA discs were gently rinsed with ultrapure water and shaken in a plate vertical shaker to obtain experimental conditions unambiguous to those described in above sections. After shaking, HA discs were rinsed and dried at room temperature.

Analysis of microbial-induced alterations on HA discs

HA discs subjected to the procedures of biofilm culturing and removal were covered with gold using a Quorum sputter and examined under a Zeiss EVO MA25 SEM under initial 200x magnification. This approach allowed us to divide HA discs into 40 fields of vision and to track alterations of ≤5μm size. Magnification was increased to observe alterations in a more detailed manner. During the course of experimentation, 6 distinct types of alterations were consistently observed and were designated as: 1) cavities, 2) pits, 3) deep recesses, 4) vast depressions, 5) spherules, and 6) acclivities based on morphologic appearance. The number of qualitative alterations of specific types identified on HA disc surfaces (n=6 for each species) was summed and presented as means with standard deviation for quantitative or statistical comparisons.

Control experiments

Three types of control experiments, also 6 HA discs each, were performed to estimate the impact of detergent (saponine) and medium on the surface of HA discs. The following discs were analysed:

- Native HA discs later referred to as “negative control 1” or “NC1”.
- HA discs treated with saponine as described in the section: “Strain incubation and biofilm removal”, later referred to as “negative control 2” or “NC2”.
- HA discs incubated in sterile medium for 72 hrs in conditions described in the section: “Strain incubation and biofilm removal”, and then treated with saponine; this control is later referred to as “negative control 3” or “NC3”.

All experiments concerning counting alterations on HA surfaces were repeated 6 times to obtain statistically reliable results.

Energy-dispersive x-ray spectroscopy (EDS) analysis

To determine elemental composition of alterations observed, SEM with energy dispersive x-ray spectroscopy (EDS) microanalysis attachment and an accelerating voltage of 20 kV was applied. SEM-EDS analysis was performed for all samples and specific types of alterations formed on HA surfaces.

Frequency of occurrence of specific pseudomonal-induced alterations

During the course of experimentation, it occurred that the pseudomonal strain caused a unique type of alteration to the HA surface in addition to other alterations, which we refer to as pseudomonal acclivities. As no similar alterations were observed in the discs coated with biofilm of other species, we aimed to assess the frequency of these alterations. Thus, the 20 clinical *P.aeruginosa* strains were allowed to form biofilm on HA discs in conditions previously described. For controls, 20 clinical strains of *S.aureus* were also cultured.

pH assessment

The pH of each cell-free supernatant, was measured using a universal pH-indicator (Merck, Poland); pH assessments were taken after 24, 48 and 72 hrs of strain incubation in the presence of HA disc.

Planimetry of HA alterations

3D computerized planimetry assessments were conducted using confocal microscopy (OLYMPUS LEXT, OLS4000) at maximum magnification of 2080x and 0.12μm × 0.01μm XY resolution. 3D parameters were estimated using algorithms for 2D analysis according to the PN-EN ISO 4287 and 4288 norms, which are standards for the assessment and profiling of surface texture in geometric planes.

Two-dimensional analysis of observed alterations

For 2D analysis of observed alterations, the geometric size assessment function of SEM analysis was applied. Using formulas of the designation of Feret's diameter, the total area of

examined objects was determined in 2D space, based on the analysis of the objects identified in the longitudinal plane.

Statistical analysis

Statistical calculations were performed using Sigma-Stat 2.0 (SPSS Inc., Chicago, Illinois). A power analysis was performed for sample size estimation prior to experimentation. ANOVA was used to test for significance between treatment and control groups. Statistical significance was defined as $P \leq 0.05$.

3. RESULTS

The manufacture of HA discs displaying smooth and regular surfaces without defects was a prerequisite condition for performing bias-free assessments concerning the potential ability of microorganisms to alter HA structure. Technology applied allowed us to produce HA discs with smooth surfaces and no defects or signs of internal porosity, which was proven by means of microtomographic techniques as shown in **Figure 1**. We were able to achieve a voxel size of 13 microns for slice-by-slice analysis of HA discs in various planes to confirm fabrication without defects. All experimental strains were able to form mature biofilm structures on the surface of manufactured HA discs [**Figure 2, Table 1**]. Quantitation of biofilm-forming cells or cfu/mm^2 on HA surface after 72 hrs of incubation is given in **Table 2;** micro-CT metrotomography analysis allowed for the surface area calculations of HA as presented in this data.

SEM evaluation of HA discs revealed presence of alterations in HA structure by both biofilm and cell-free supernatants. Characteristic morphologic perturbations of HA surfaces were observed in all samples. Observed alterations were classified into specific morphologic subtypes as described in **Table 3**. There were species-specific alterations (pits, spherules, acclivities) and species-unspecific alterations (cavities, deep recesses, vast depressions). The mean number of alterations observed for all morphologic subtypes is given in **Table 4**. Photographic examples of each type of alteration are presented in **Figure 3.** The number of alterations caused by microbes on HA surfaces was statistically significantly higher compared to all types of controls [NC1,2,3]; this was true not only for HA discs incubated with cells as shown in **Figure 4**, but also with cell-free supernatant as shown in **Figure 5**. The highest number of alterations observed occurred when HA discs were colonized by mixed biofilms of *C.albicans* + *S.mutans*. *S. mutans* biofilm incubated in BHIM+3%S was the most detrimental to HA surfaces among single-species biofilms. The impact of media composition on this organisms' ability to alter HA was also observed. Mean number of alterations caused by *Str.mutans* incubated in BHIM+3%S was over 2x higher as compared to the number of alterations caused by this jaw pathogen cultured in the same medium without additional sugar content [**Figure 4**, **Figure 5**].

When comparing biofilm versus cell-free supernatants, there was no statistically significant difference in ability to alter HA surfaces as shown in **Figure 6**. The results of pH changes over time are presented in **Table 5**. The pH of the sterile media applied was near neutral value. The majority of tested strains acidified the environment, the only exception was *P.aeruginosa*. Though unique in terms of pH value, this bacterial species was able to cause

more damage to HA surfaces than acidifying *S.aureus*, *C.albicans* and *S.mutans* incubated without additional sugar content. One of the types of alterations observed, called acclivities, was produced only by *P.aeruginosa*. Only this type of alteration was an elevation of HA while all other alterations were declivities. Acclivity size was exceptional, and could be easily seen with a magnifying glass, whereas the rest of the alterations required SEM to observe them. To assess the frequency of the occurrence of acclivities, 20 clinical *P.aeruginosa* strains were allowed to form biofilm on 20 HA discs; acclivities were found in 6 of 20 HA discs (33%).

SEM-EDS analysis of control versus experimental HA discs revealed that all biofilm-induced alterations of HA had an elemental composition that resembled that of intact or control HA. **Figure 7** shows an example of SEM-EDS analysis for a pseudomonal acclivity, while **Figure 8** shows an example of a pseudomonal cavity evaluated by computerized planimetry.

4. DISCUSSION

Normal bone remodelling involves a complex interplay of osteoclasts and osteoblasts in cycles of resorption and reconstitution. Cytokines (e.g. interleukin-1, interleukin-6, interleukin-11, and tumor necrosis factor) generated locally by bone cells and also inflammatory cells are potent osteolytic factors.[1] During bone infection, phagocytes attempt to contain invading microorganisms and, in the process, generate toxic oxygen radicals and release proteolytic enzymes that lyse surrounding tissues.[1] Several bacterial components such as endotoxin-lipopolysaccharide, lipoteichoic acid, and fimbriae can act directly or indirectly as bone-resorbing factors.[13] The presence of arachidonic acid metabolites, such as prostaglandin E2, which is a strong osteoclast agonist, decreases the amount of the bacterial inoculum needed to produce infection.[1]

To date, the possibility of direct bone resorption by biofilm pathogens has not been seriously considered or elucidated. Direct bone destruction by pathogens *in vivo* could allow for invasion of organisms into deeper tissues to evade host immune responses, gain access to eukaryotic cells, or spread hematogenously and reach more viable sites for colonisation and access to nutrition.[14] For example, the bone pathogen *S.aureus* is internalized by bone cells and it has been suggested that this ability enables the bacterium to avoid the host immune system and/or antibiotic treatment.[15]

Therefore, the purpose of this study was to evaluate the potential of biofilm pathogens in the absence of inflammation to alter HA surfaces to which they bind and colonise during clinical bone infections such as osteomyelitis, periodontitis, and jaw osteonecrosis. We observed that in the absence of host immunity or osteoclastogenesis, all biofilm pathogens in our study could damage and resorb HA surfaces, causing characteristic and reproducible morphologic changes. Surface changes identified may in some cases be part of a continuum of damage. For example, small pits or depressions may progress to larger lesions such as deep recesses and cavities. A deep recess may be an intermediate state of cavities, where initially there is an intact surface in a region that similar to a landslide becomes loose and gives way to a large cavity.

Spectroscopy of control versus experimental HA discs revealed that all biofilm-induced alterations of HA had a chemical composition that resembled that of intact or control HA, and therefore do not represent remnant biofilm material, structures or contaminants. Further, when comparing biofilm versus cell-free supernatants, there was no statistically significant difference in ability to alter HA surfaces. This suggests that extracellular or cell-free factors are responsible for HA damage, such as biofilm matrix or acid/base liberation, as opposed to direct damage by cells.

The majority of tested strains acidified the environment; the only exception was *P.aeruginosa*. Though unique in terms of pH value being basic, this bacterial species was able to cause significant damage to HA surfaces and more than acidifying *S.aureus*, *C.albicans* and *S.mutans* incubated without additional sugar content. This could suggest that there is no direct correlation between pH value and ability to cause HA destruction, or more likely that other factors play important roles in this pathophysiologic process. As there is robust evidence that low pH is one of the major factors responsible for the cariogenic potential of *S.mutans* and its ability to destroy hard tissues such as tooth enamel (which is also avascular like sequestra), results obtained in this study for *P.aeruginosa* indicate that other mechanisms may also be involved in hard tissue destruction. Further, *P.aeruginosa* acclivities suggest that perhaps chemical processes like chelation or precipitation of HA occur, which may be driven by basic pH conditions as opposed to acidic conditions which result in HA dissolution.

We further observed that mixed-species biofilms caused more HA destruction than single-species biofilms. This correlates with clinico-pathologic findings of co-aggregation of bacteria (streptococci) and yeast (candida) from specimens of jaw osteonecrosis,[6,10] a condition where significant bone loss occurs, suggesting synergistic effects of mixed organisms. Importantly, the HA resorption pattern which was observed in this study was dissimilar to osteoclast-associated resorption pits which have characteristic trails and size.[16] Osteoclasts have a specific cytoskeletal structure, the podosome, which is crucial for the degradation of HA. To resorb bone, osteoclasts polarize and actively secrete protons and proteases into a resorption pit where these molecules are confined by a podosome-containing sealing zone.[17] The resorption pits observed in this study did not have characteristic trails and size that would be expected for osteoclastogenesis-related bone resorption, which is understandable given the lack of osteoclasts in our experimental design, and which indicates that resorptive pits can be formed by pathogens alone.

Our findings suggest that mechanisms for HA alteration may involve acid/base reactions. However, other processes may be involved such as oxidation/reduction reactions on the HA surface. HA surface changes induced by biofilms may be similar to processes utilized by metal corroding biofilms.[18] HA may also serve as a solid pH buffer and consume protons, a process leading to its dissolution. Electromicrobiology has provided insights recently into surface electrochemical activity of biofilms and their potential for changing surface topography, which could play a role in the pathophysiology of chronic bone infections.[19,20] In future studies, we will further explore the mechanisms and factors responsible for HA alterations by pathogens by using clinical bone samples and performing *ex vivo* studies with

mixed-species biofilms associated with bone infections. We will also utilize non-pathogenic biofilm organisms as controls in future studies to further test our hypothesis.

A paradigm shift may be required for future studies in this field as infectious disease states of bone may involve direct microbial resorption of bone in addition to immune-mediated destruction. In the human body, rather than representing a static community relying on host immunity and eukaryotic cell recruitment, biofilms may be dynamic superorganisms that can also independently alter the surfaces they inhabit, such as HA in chronic bone infections. This work represents a necessary first-step for demonstrating proof of principle. The extent and clinical significance of direct bone resorption by biofilms remains unclear and requires further investigation. Importantly, the *in vitro* nature of the current study and its inherent limitations do not allow for direct translation of our findings to the clinical setting or to clinical practice. Nonetheless, these findings may have important translational implications in the future for the pathogenesis of chronic bone infections and for targeted antimicrobial therapeutics in infectious bone disease.

Acknowledgments

This work was made possible by grant number L32MD003617 from the NIH (NIMHD) in addition to a seed grant from the University of Southern California, Ostrow School of Dentistry.

REFERENCES

1. Stoodley P, Ehrlich GD, Sedghizadeh PP, et al. Orthopaedic biofilm infections. Curr Orthop Pract. 2011; 22(6):558–63. [PubMed: 22323927]
2. Donlan RM, Costerton JW. Biofilms: Survival mechanisms of clinically relevant microorganisms. Clin Microbiol Rev. 2002; 15:167–93. [PubMed: 11932229]
3. Lew DP, Waldvogel FA. Osteomyelitis. Lancet. 2004; 364(9431):369–79. [PubMed: 15276398]
4. Schaudinn C, Gorur A, Keller D, et al. Periodontitis: an archetypical biofilm disease. J Am Dent Assoc. 2009; 140(8):978–86. [PubMed: 19654249]
5. Sedghizadeh PP, Kumar SK, Gorur A, et al. Microbial biofilms in osteomyelitis of the jaw and osteonecrosis of the jaw secondary to bisphosphonate therapy. J Am Dent Assoc. 2009; 140(10): 1259–65. [PubMed: 19797556]
6. Souza PP, Lerner UH. The role of cytokines in inflammatory bone loss. Immunol Invest. 2013; 42(7):555–622. [PubMed: 24004059]
7. Jiao Y, Darzi Y, Tawaratsumida K, Marchesan JT, et al. Induction of bone loss by pathobiont-mediated Nod1 signaling in the oral cavity. Cell Host Microbe. 2013; 13(5):595–601. [PubMed: 23684310]
8. Ruggiero SL, Dodson TB, Assael LA, et al. American Association of Oral and Maxillofacial Surgeons Position Paper on Bisphosphonate-Related Osteonecrosis of the Jaws-2009 Update. J Oral Maxillofac Surg. 2009; 67:2–12. [PubMed: 19371809]
9. Sedghizadeh PP, Kumar KSS, Gorur A. Identification of microbial biofilms in osteonecrosis of the jaws secondary to bisphosphonate therapy. J Oral Maxillofac Surg. 2008; 66:767–75. [PubMed: 18355603]
10. Kumar SK, Gorur A, Schaudinn C, et al. The role of microbial biofilms in osteonecrosis of the jaw associated with bisphosphonate therapy. Curr Osteoporos Rep. Mar. 2010; 8(1):40–8. [PubMed: 20425090]
11. Brady RA, Leid JG, Calhoun JH, et al. Osteomyelitis and the role of biofilms in chronic infection. FEMS Immunol Med Microbiol. 2008; 52(1):13–22. [PubMed: 18081847]

12. Kos M, Junka A, Smutnicka D, et al. Pamidronate enhances bacterial adhesion to bone hydroxyapatite. Another puzzle in the pathology of bisphosphonate-related osteonecrosis of the jaw? J Oral Maxillofac Surg. 2013; 71(6):1010–6. [PubMed: 23489958]
13. Nair SP, Meghji S, Wilson M, et al. Bacterially induced bone destruction: mechanisms and misconceptions. Infect Immun. 1996; 64(7):2371–80. [PubMed: 8698454]
14. Khalil H, Williams RJ, Stenbeck G, et al. Invasion of bone cells by Staphylococcus epidermidis. Microbes Infect. 2007; 9(4):460–5. [PubMed: 17331787]
15. Reilly SS, Hudson MC, Kellam JF. In vivo internalization of Staphylococcus aureus by embryonic chick osteoblasts. Bone. 2000; 26:63–70. [PubMed: 10617158]
16. Rumpler M, Würger T, Roschger P, et al. Osteoclasts on bone and dentin in vitro: mechanism of trail formation and comparison of resorption behavior. Calcif Tissue Int. 2013; 93(6):526–39. [PubMed: 24022329]
17. Georgess D, Machuca-Gayet I, Blangy A, et al. Podosome organization drives osteoclast-mediated bone resorption. Cell Adh Migr. 2014; 7:8.
18. Zuo R. Biofilms: strategies for metal corrosion inhibition employing microorganisms. Appl Microbiol Biotechnol. 2007; 76:1245–53. [PubMed: 17701408]
19. Ishii S, Suzuki S, Norden-Krichmar TM, et al. Microbial population and functional dynamics associated with surface potential and carbon metabolism. ISME J. 2014; 8(5):963–78. [PubMed: 24351938]
20. Wanger G, Gorby Y, El-Naggar MY, et al. Electrically conductive bacterial nanowires in bisphosphonate-related osteonecrosis of the jaw biofilms. Oral Surg Oral Med Oral Pathol Oral Radiol. 2013; 115(1):71–8. [PubMed: 23217537]

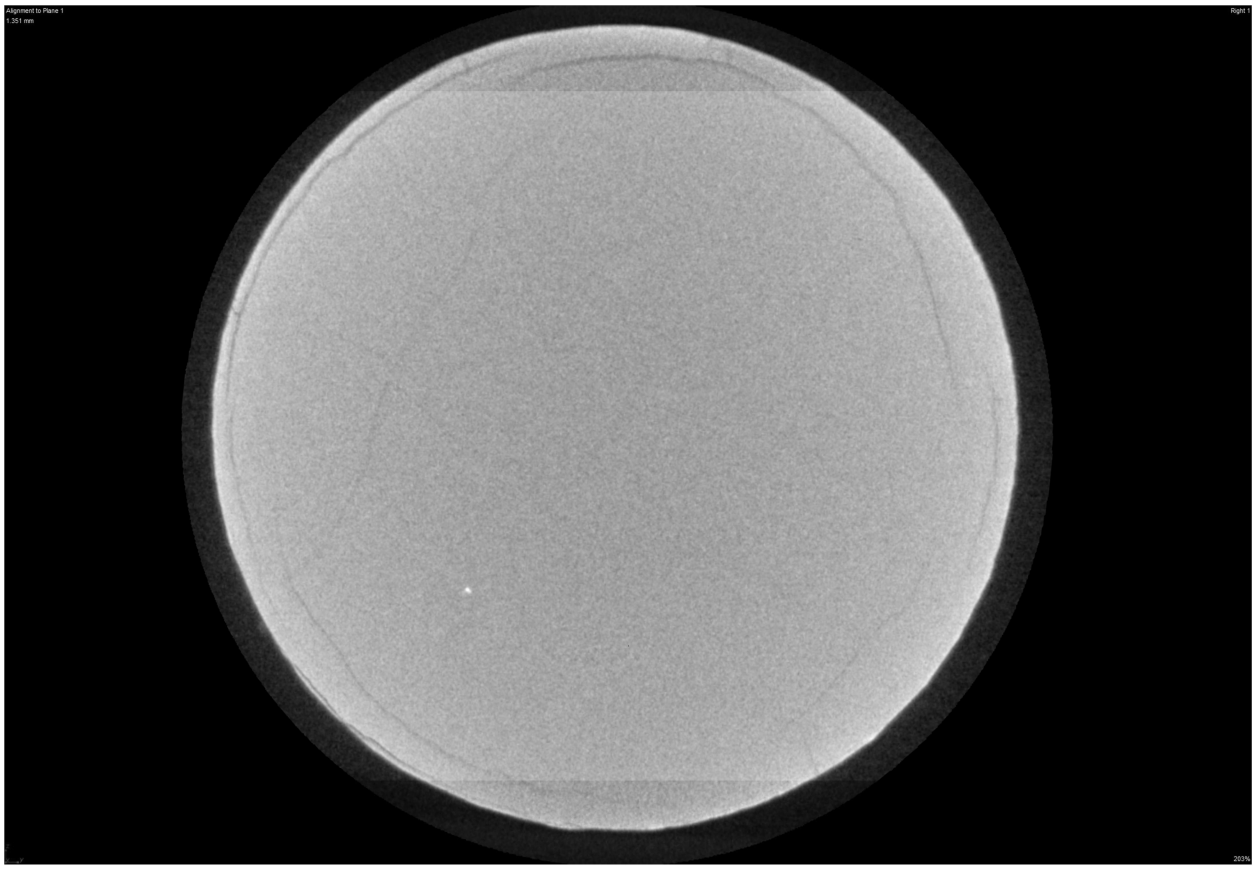

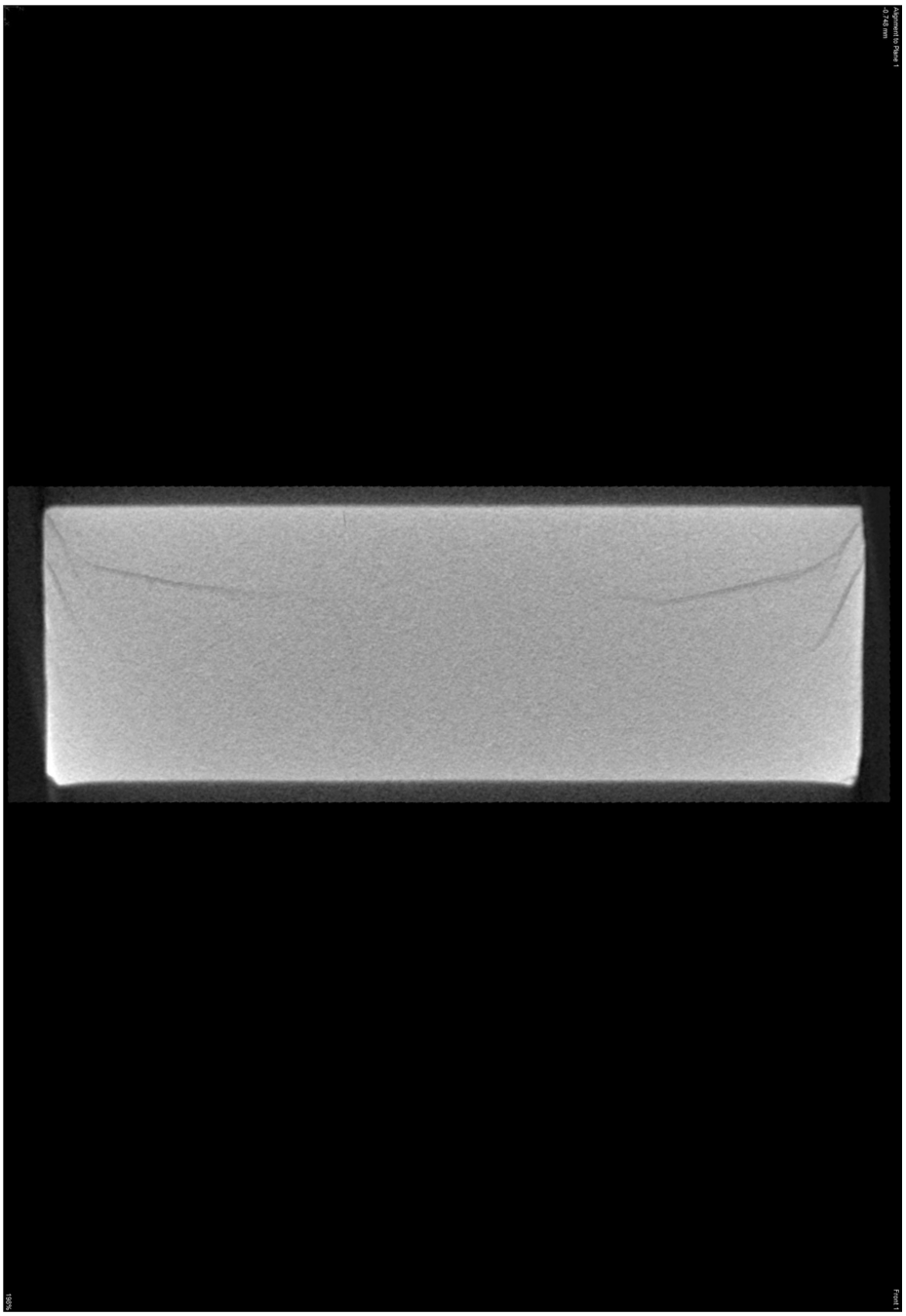

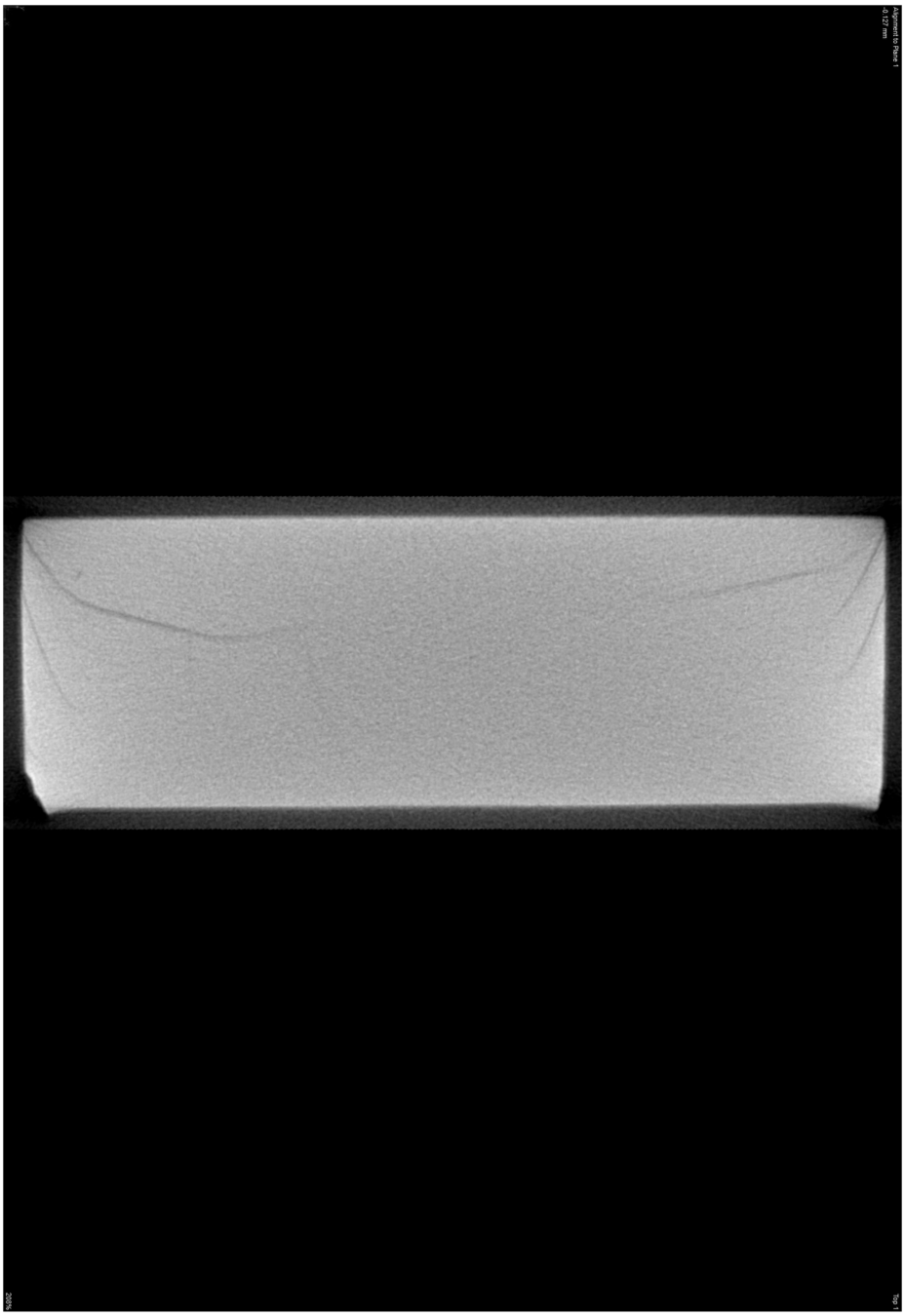

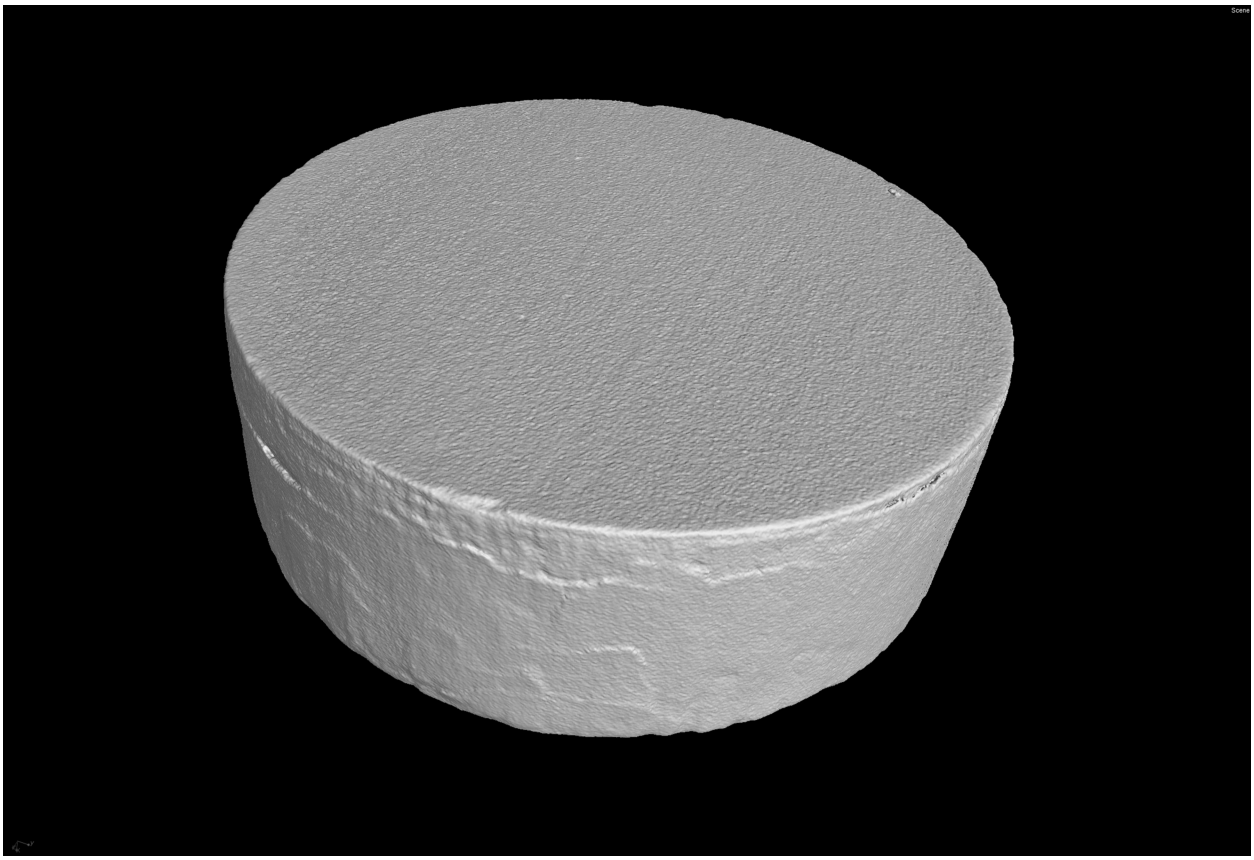

Figure 1.

A. Micro-CT images of manufactured experimental HA discs - axial section.

Figure 1B. Micro-CT images of manufactured experimental HA discs - Coronal section.

Figure 1C. Micro-CT images of manufactured experimental HA discs - sagittal section.

Figure 1D. 3D reconstruction of HA disc.

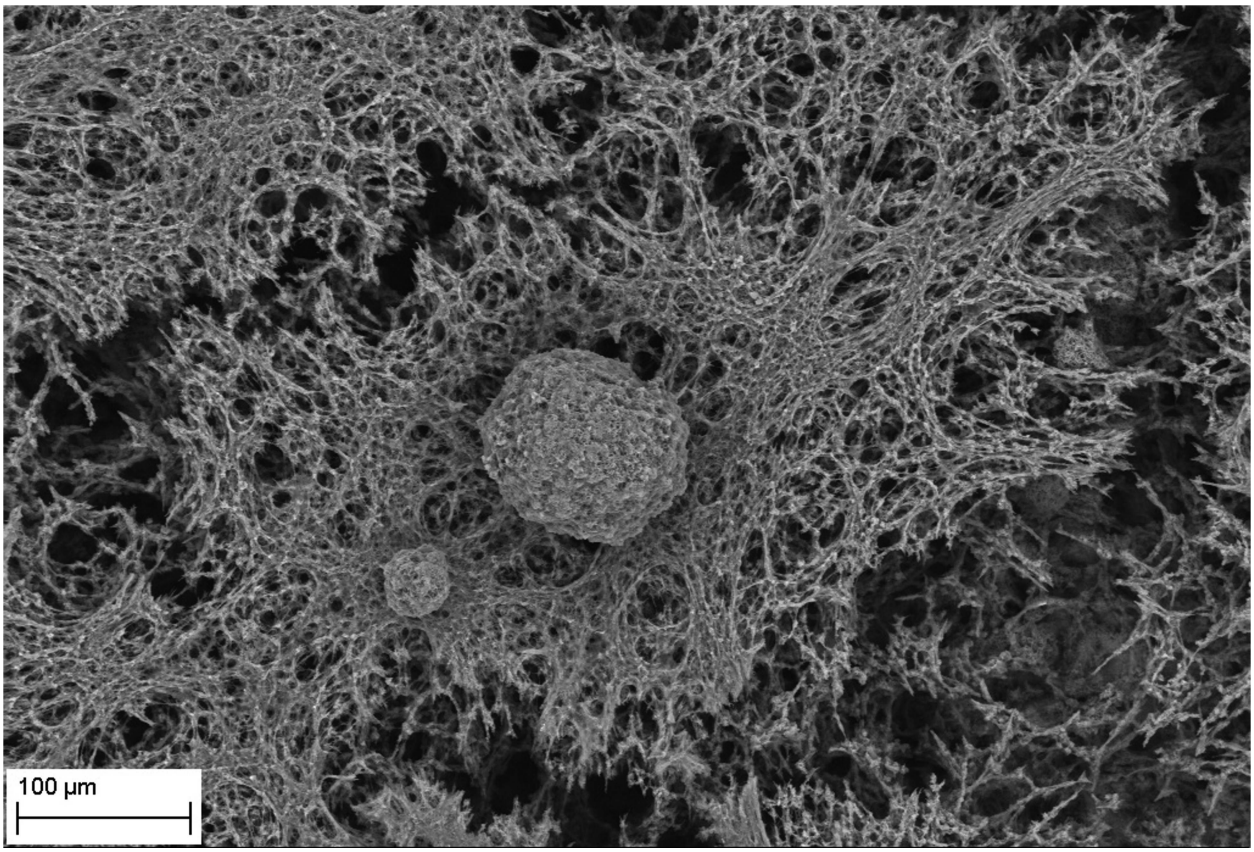

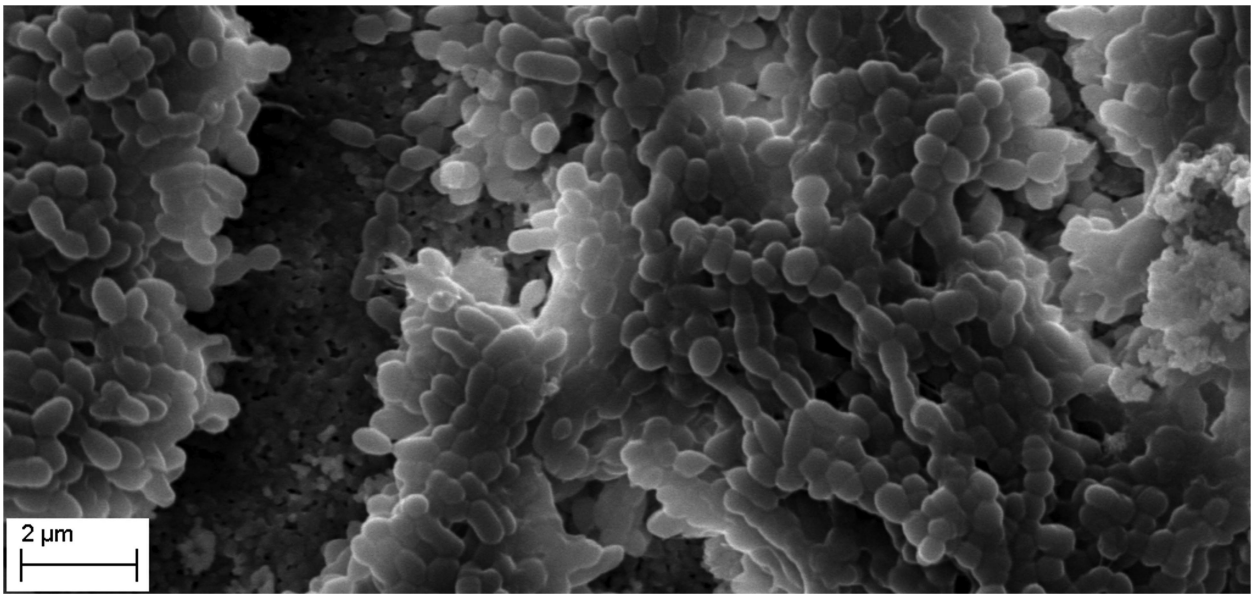

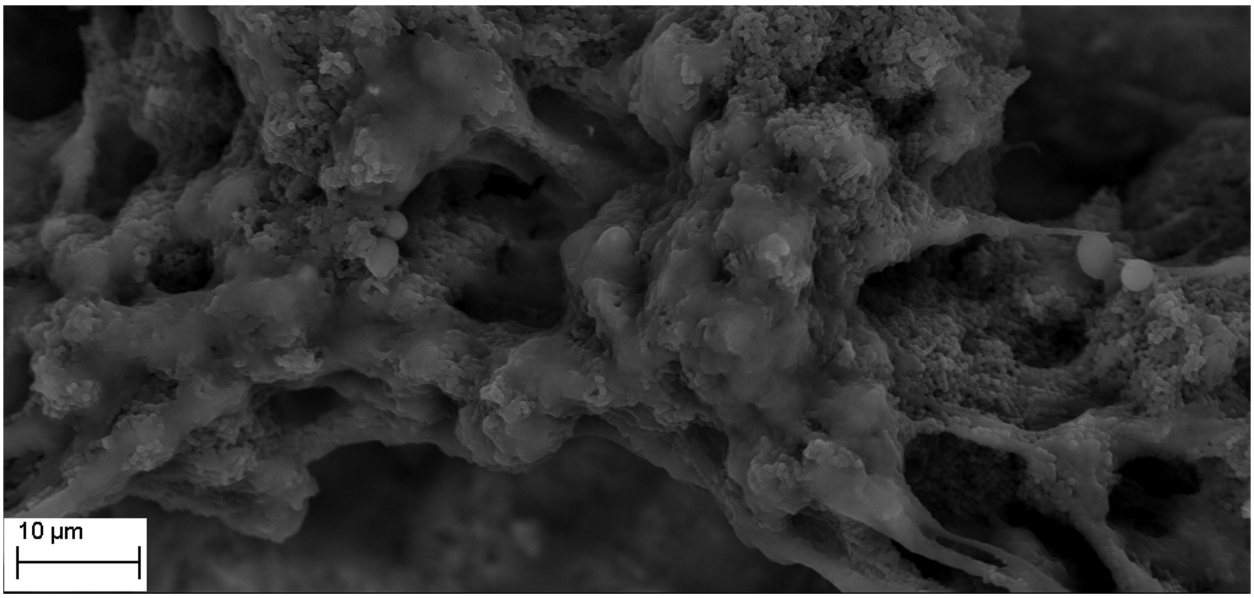

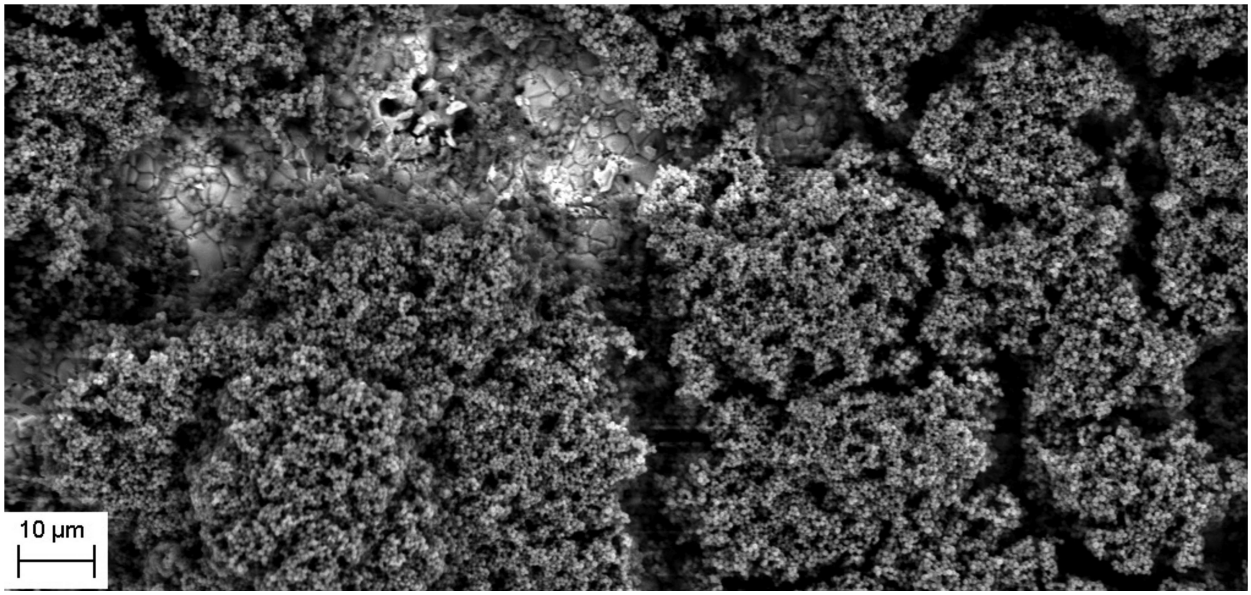

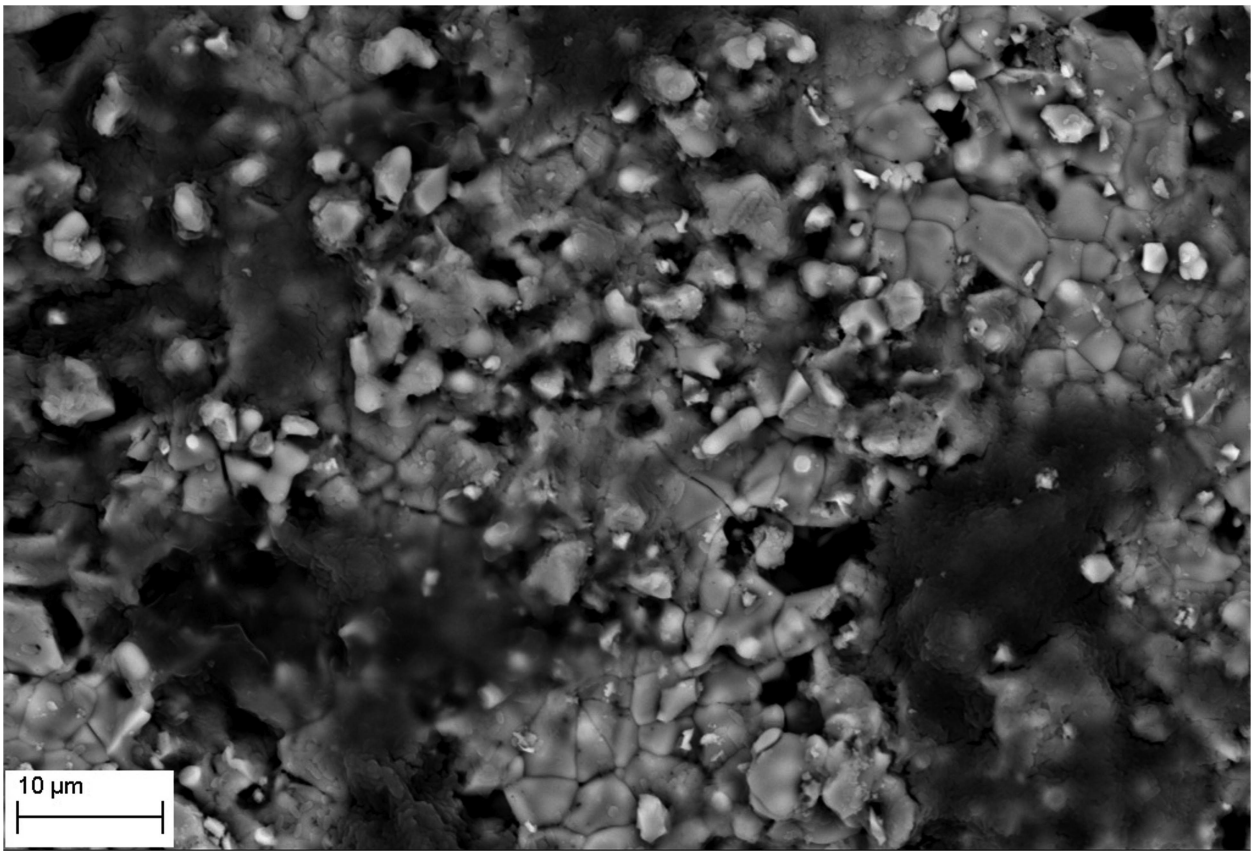

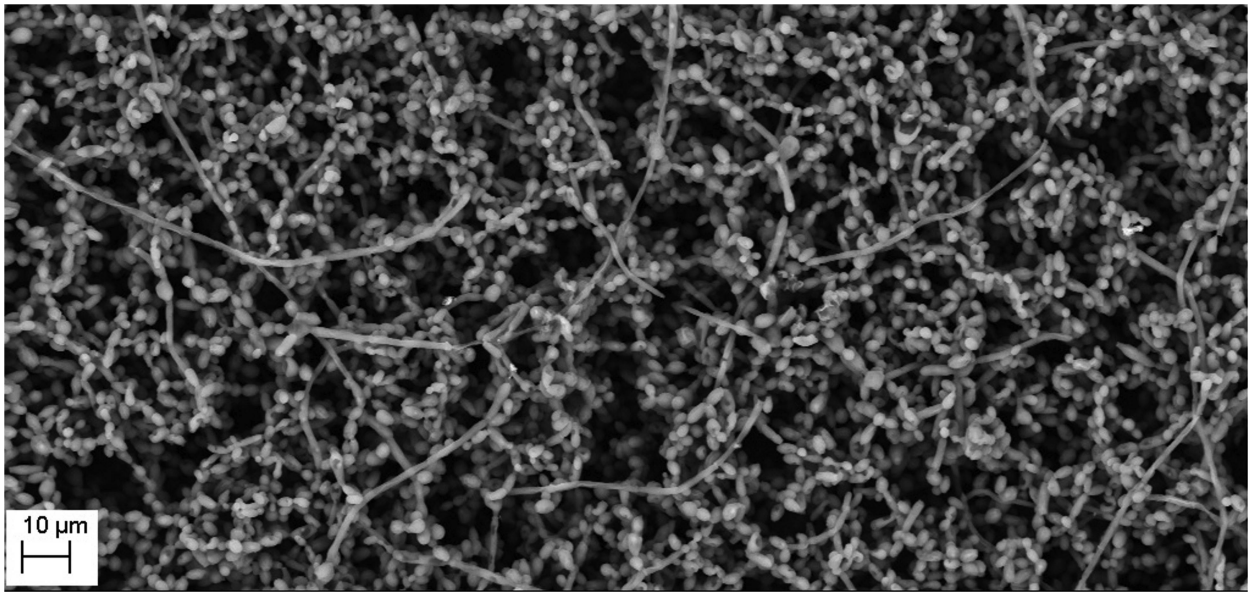

Figure 2.

A. Ability of tested strains to form biofilm on HA discs. *S.mutans* biofilm in BHIM supplemented with 3% sucrose; **Magnification:** 417x

Figure 2B. Ability of tested strains to form biofilm on HA discs. *S.mutans* biofilm in BHIM; **Magnification: B–** 13850x

Figure 2C. Ability of tested strains to form biofilm on HA discs. Mixed biofilm of *C.albicans* and *S.mutans*; **Magnification:** 2930x

Figure 2D. Ability of tested strains to form biofilm on HA discs. *S.aureus* biofilm; **Magnification:** 5060x

Figure 2E. Ability of tested strains to form biofilm on HA discs. **E** – *P.aeruginosa* biofilm. **Magnifications:** 5060x

Figure 2F. Ability of tested strains to form biofilm on HA discs. **F** - *C.albicans* biofilm. **Magnification:** 1750x.

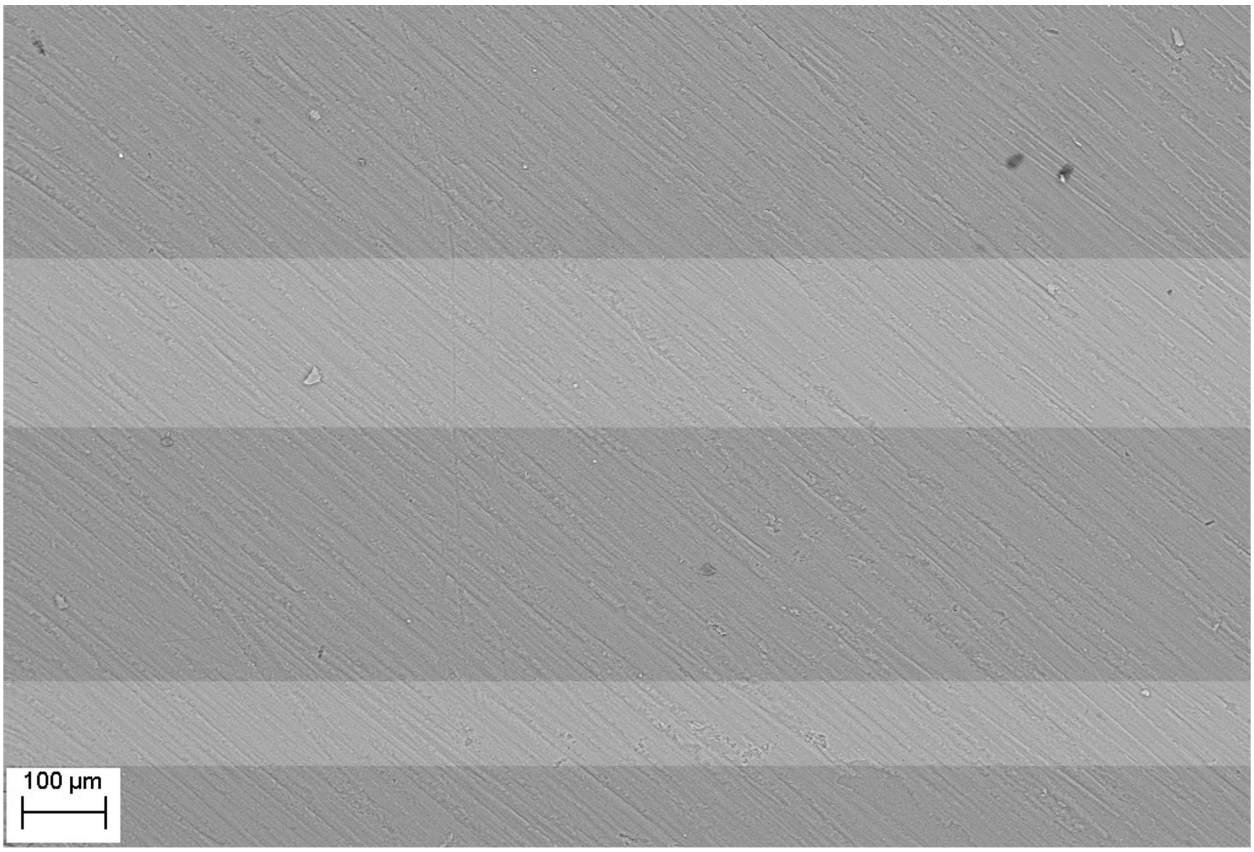

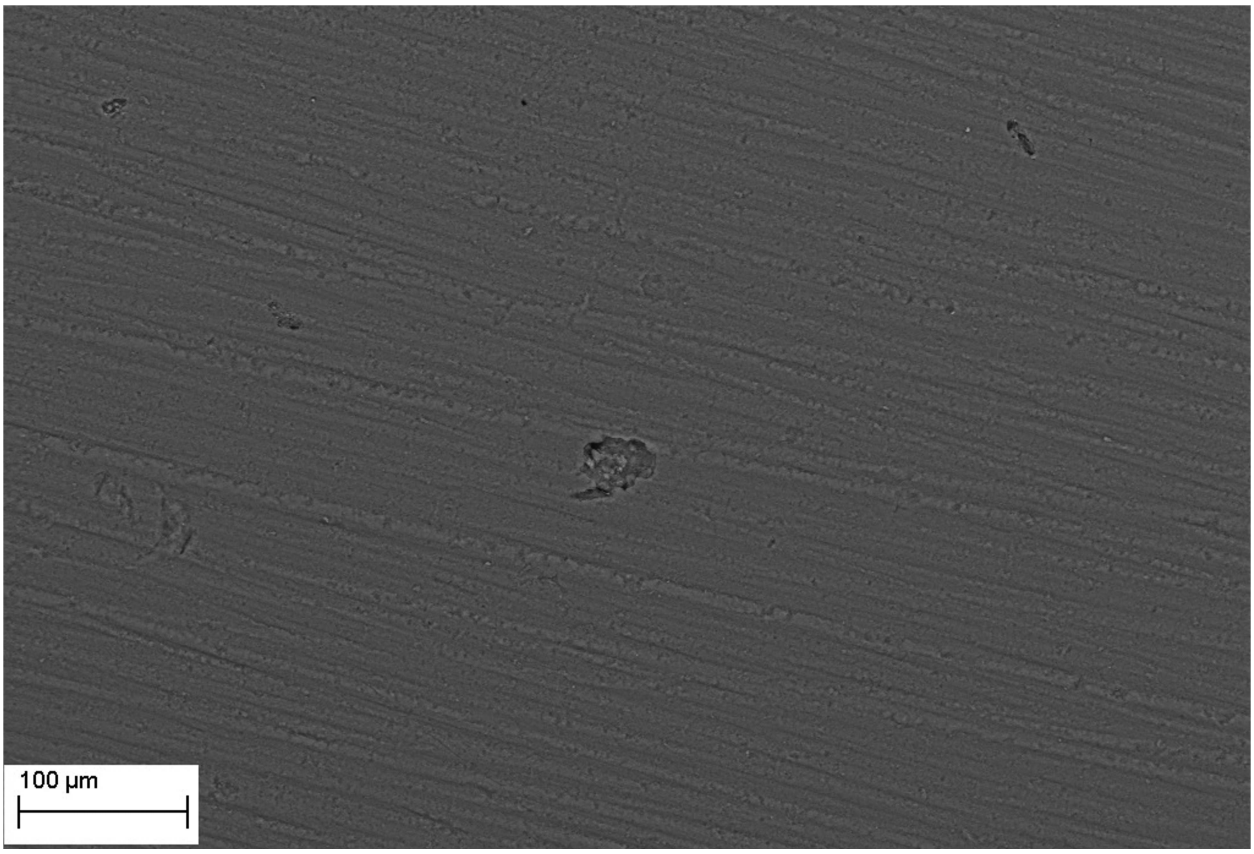

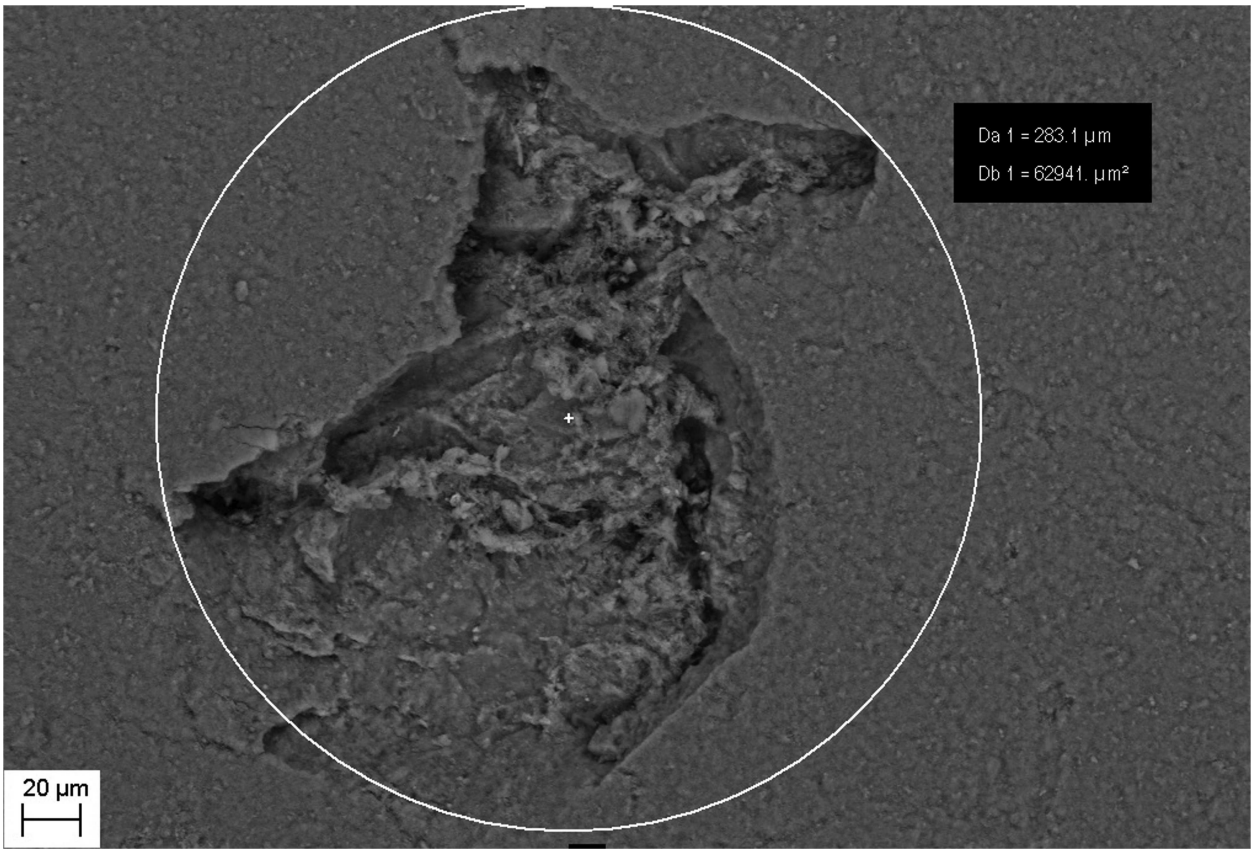

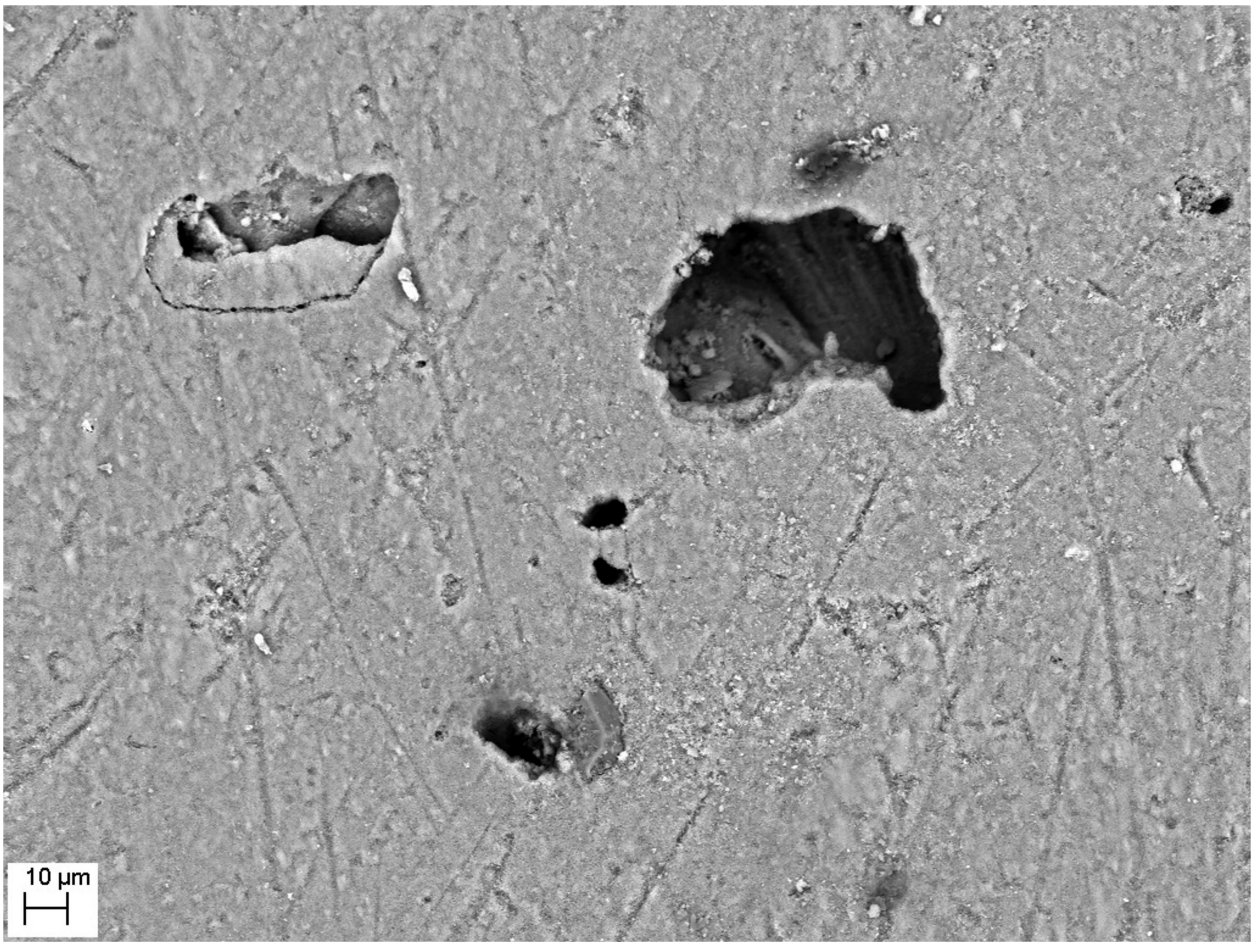

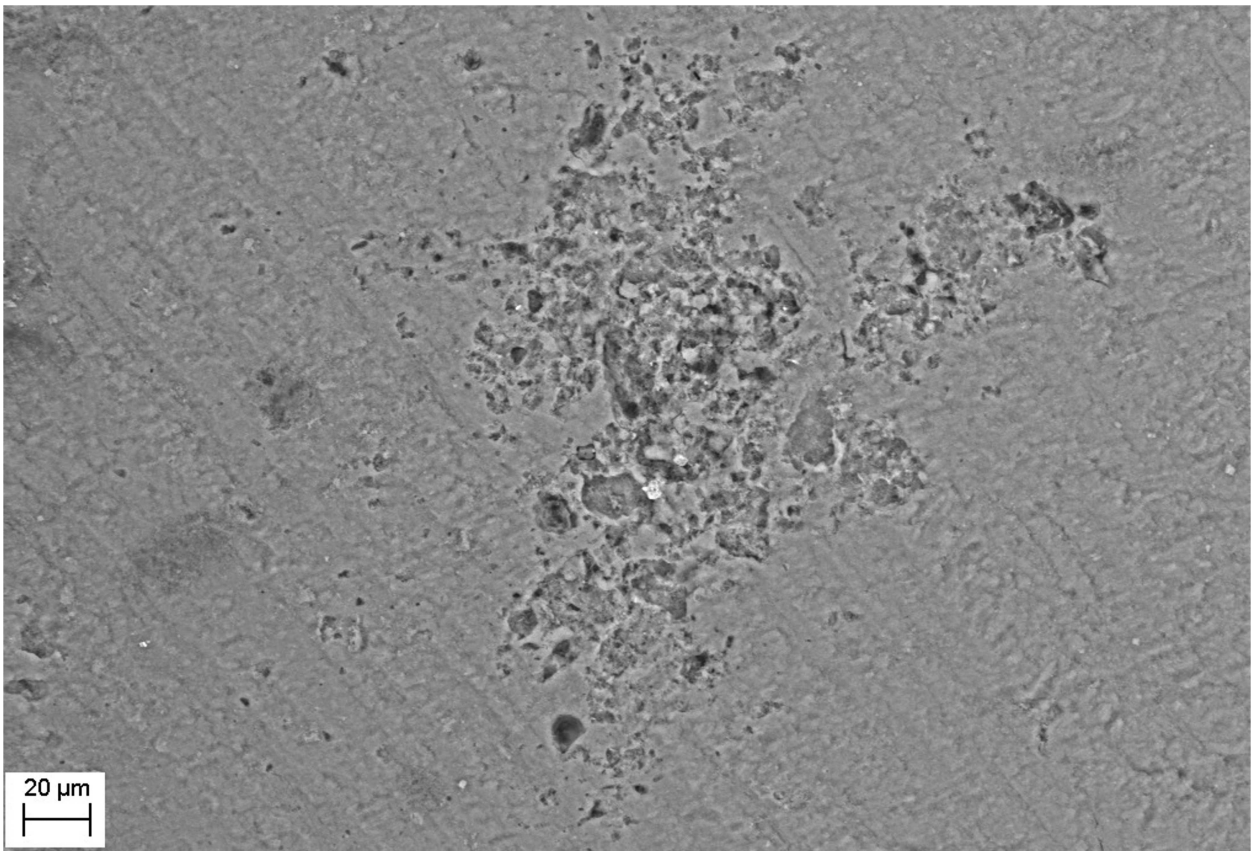

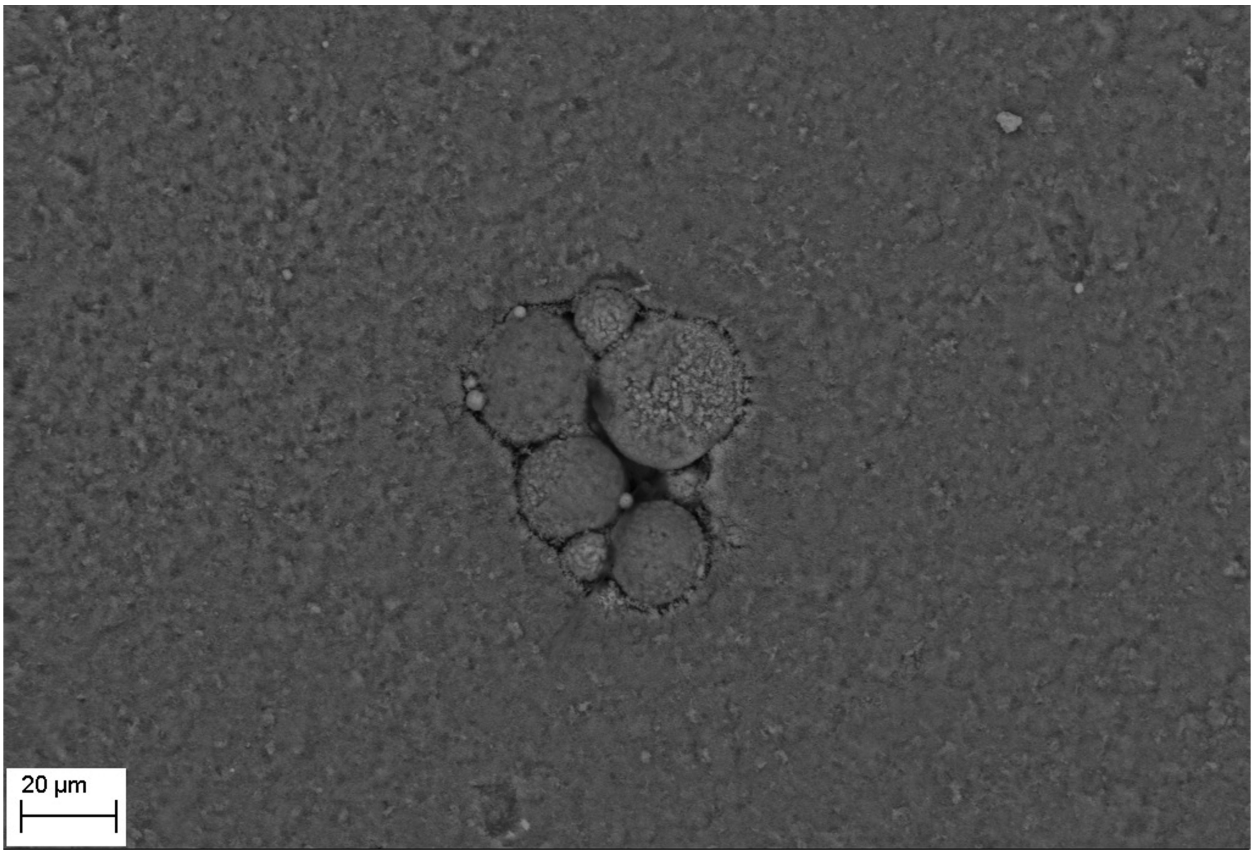

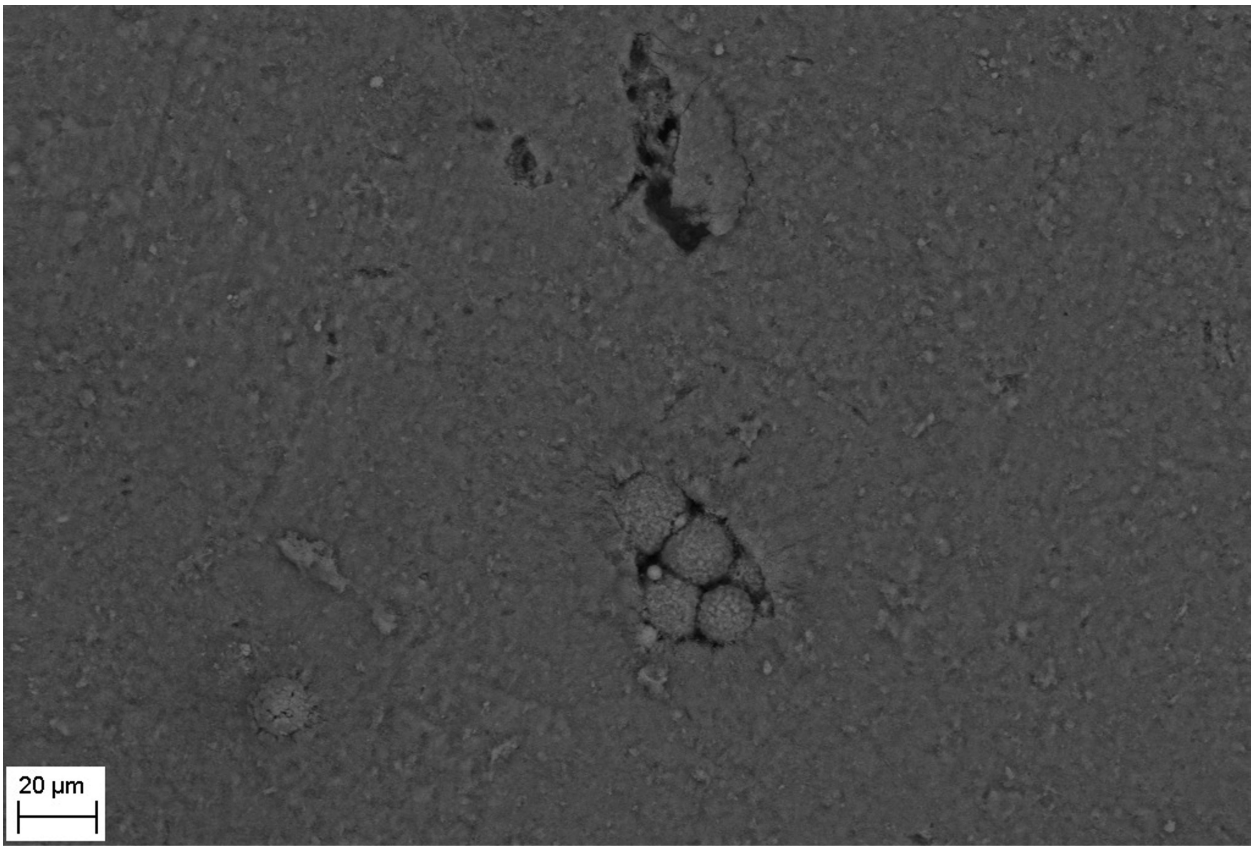

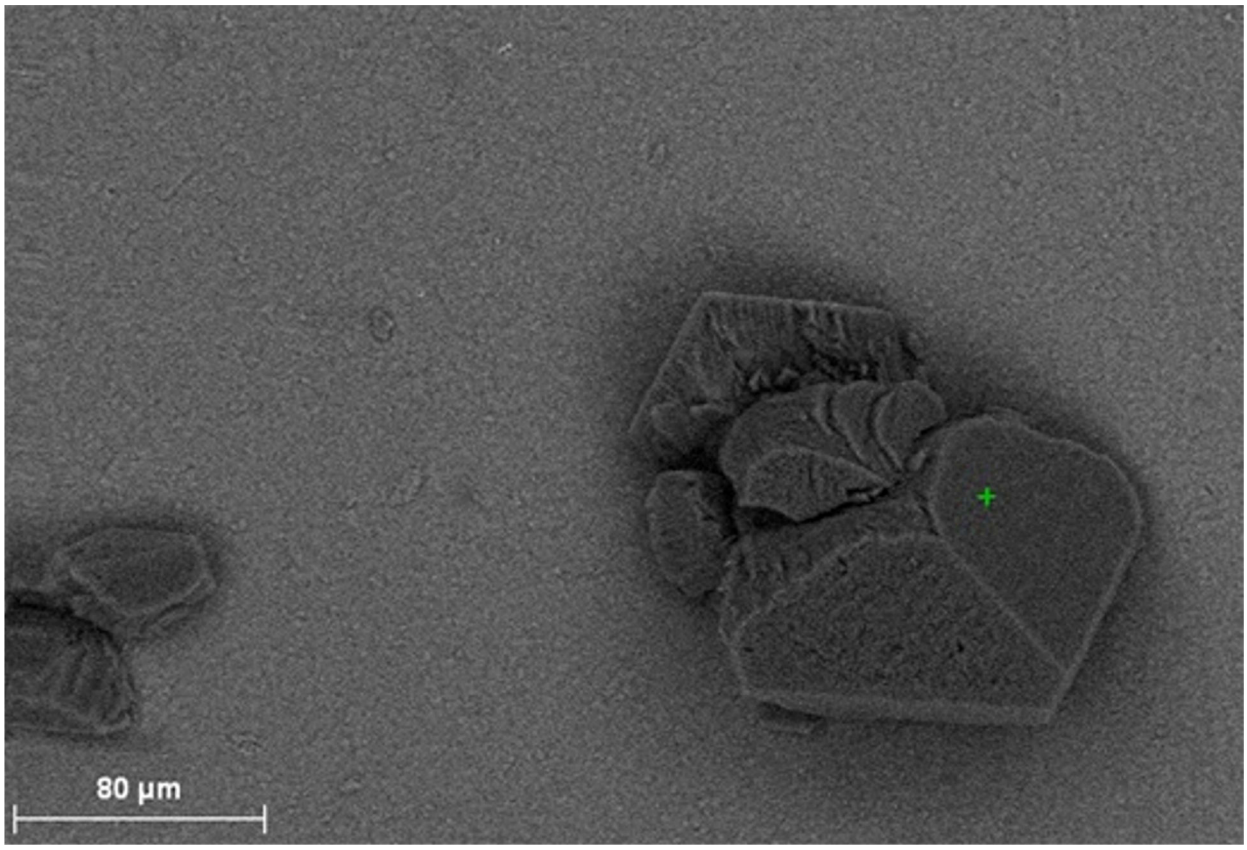

Figure 3.

A - Intact surface of HA disc.

Figure 3B - surface of HA disc incubated in TSB and treated with saponine. Single cavities are marked with arrows.

Figure 3C - cavity; *S.aureus* sample.

Figure 3D - pits (**1**), deep recess (**2**), cavity (**3**); *S.mutans* sample.

Figure 3E - vast depression; *C.albicans* sample.

Figure **3F** - spherules formed in the *S.aureus* sample.

Figure 3G - deep recess (**1**), spherules (**2**) formed in *S.mutans* sample.

Figure 3H - Acclivities formed exclusively in *P.aeruginosa* sample

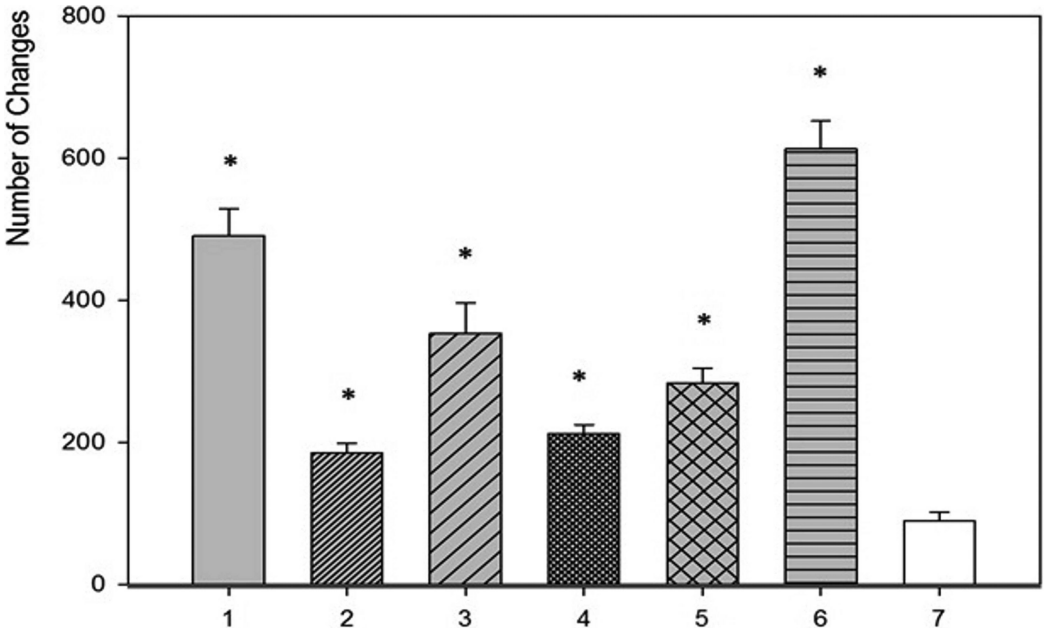

Figure 4. Number of alterations caused by biofilm of tested strains

1 – *S.mutans* (BHIM+3% sucrose); 2 - *S.mutans* (BHIM without sucrose); 3 - *P.aeruginosa;* 4 - *S.aureus*; 5 - *C.albicans*; 6 - mixed biofilm (*S.mutans* + *C. albicans*). 7 - NC3 (disc incubated in medium and treated with saponine). * -differences significant statistically, $P \leq 0.05$; One-way ANOVA test.

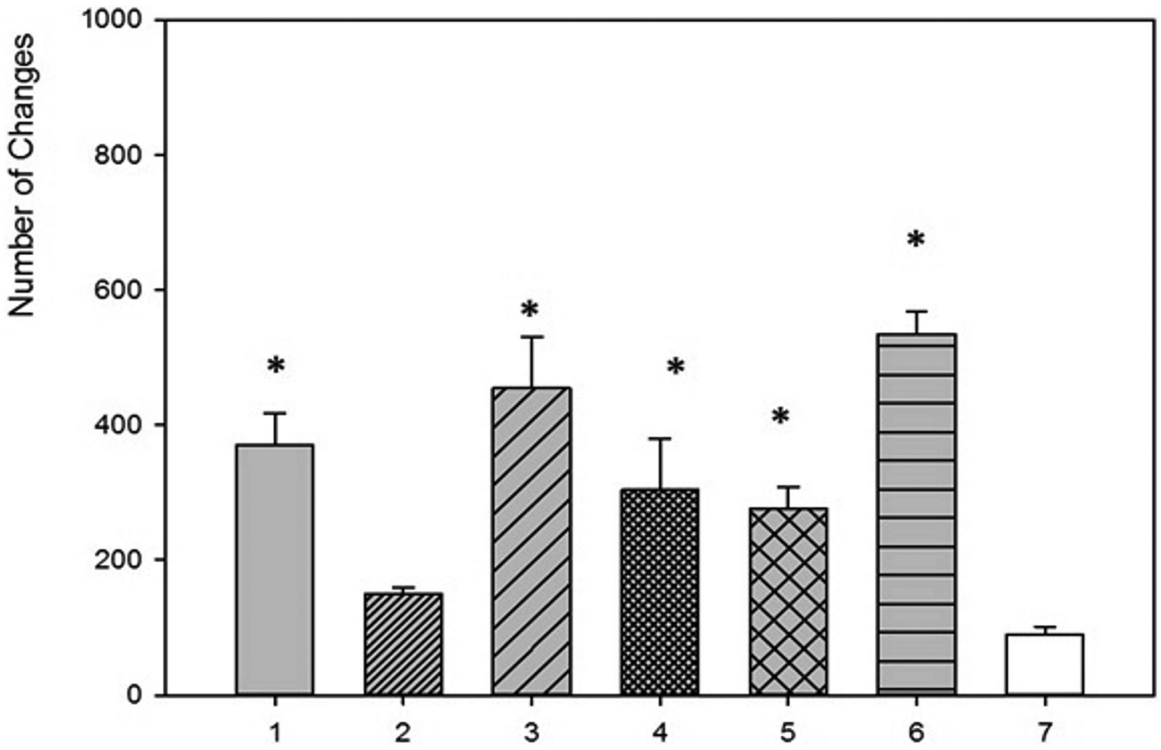

Figure 5. Number of alterations caused by cell-free supernatant

1 – *S.mutans* (BHIM+3% sucrose); 2 -*S.mutans* (BHIM without sucrose); 3 - *P.aeruginosa*; 4 - *S.aureus*; 5 - *C.albicans*; 6 - mixed biofilm (*S.mutans* + *C. albicans*). 7 -. NC3 (disc incubated in medium and treated with saponine). * -differences statistically significant, $P \leq 0.05$; One-way ANOVA test.

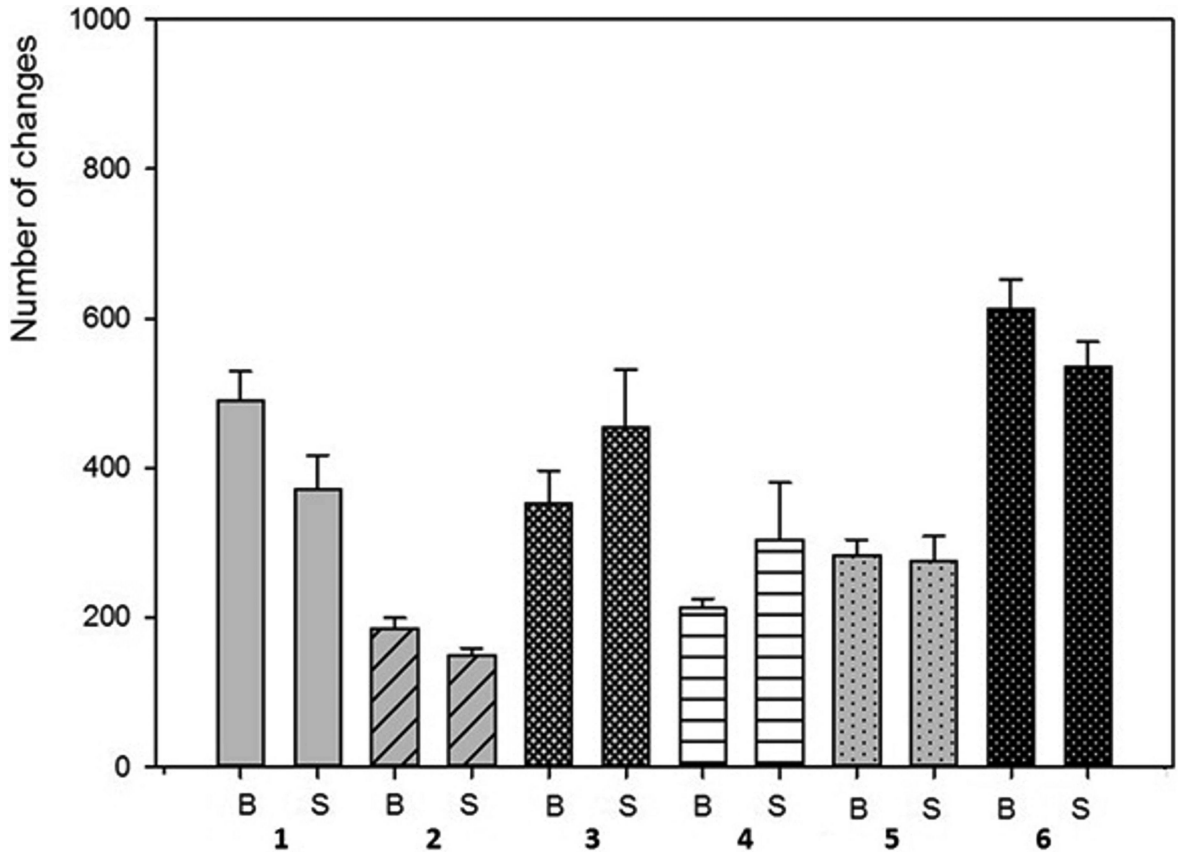

Figure 6. Comparison of number of alterations caused by biofilm [B] vs. cell-free supernatant [S]

1 – *S.mutans* (BHIM+3% sucrose); **2** - *S.mutans* (BHIM without sucrose); **3** - *P.aeruginosa*; **4** - *S.aureus*; **5** - *C.albicans*; **6** - mixed biofilm (*S.mutans*+*C.albicans*).

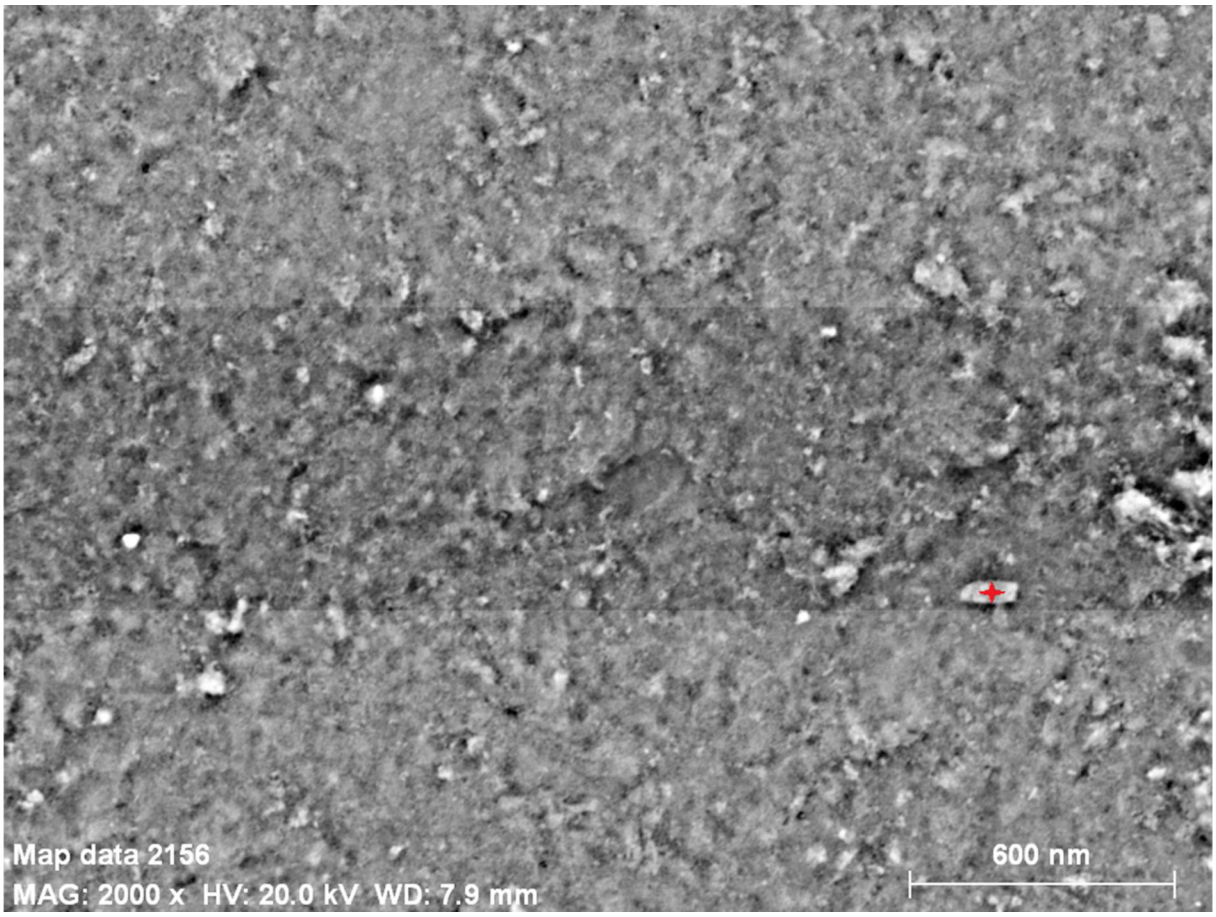

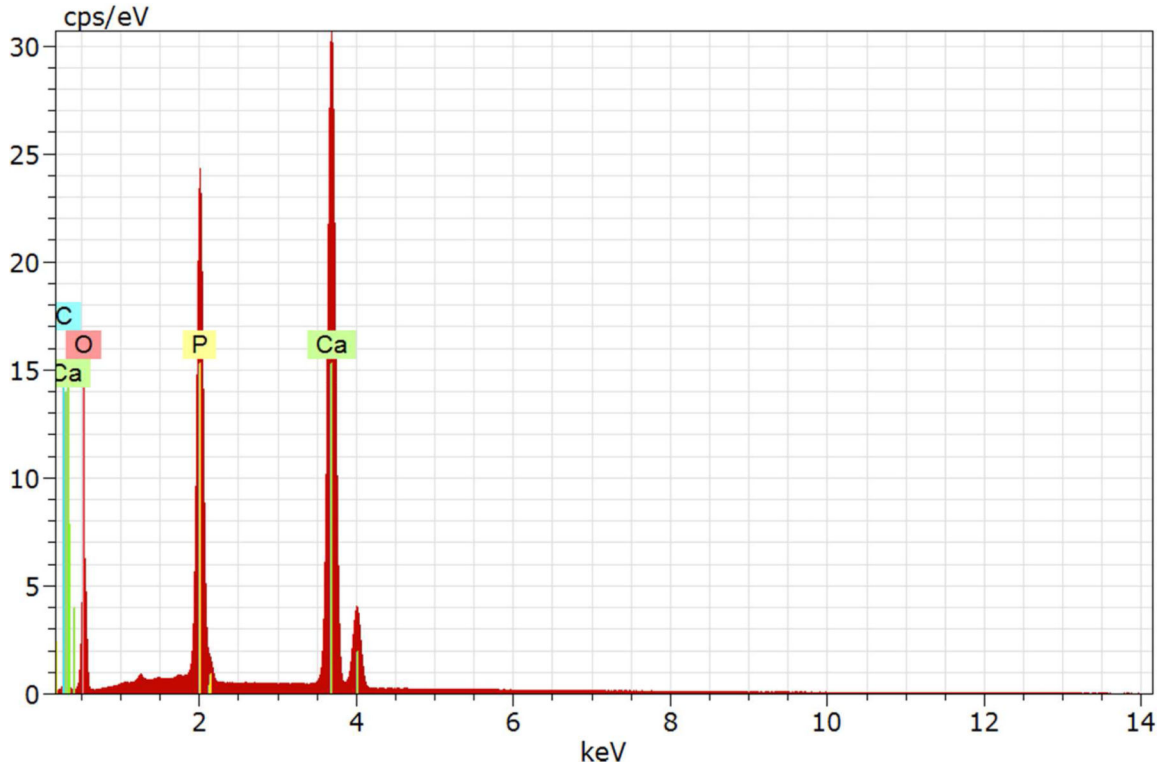

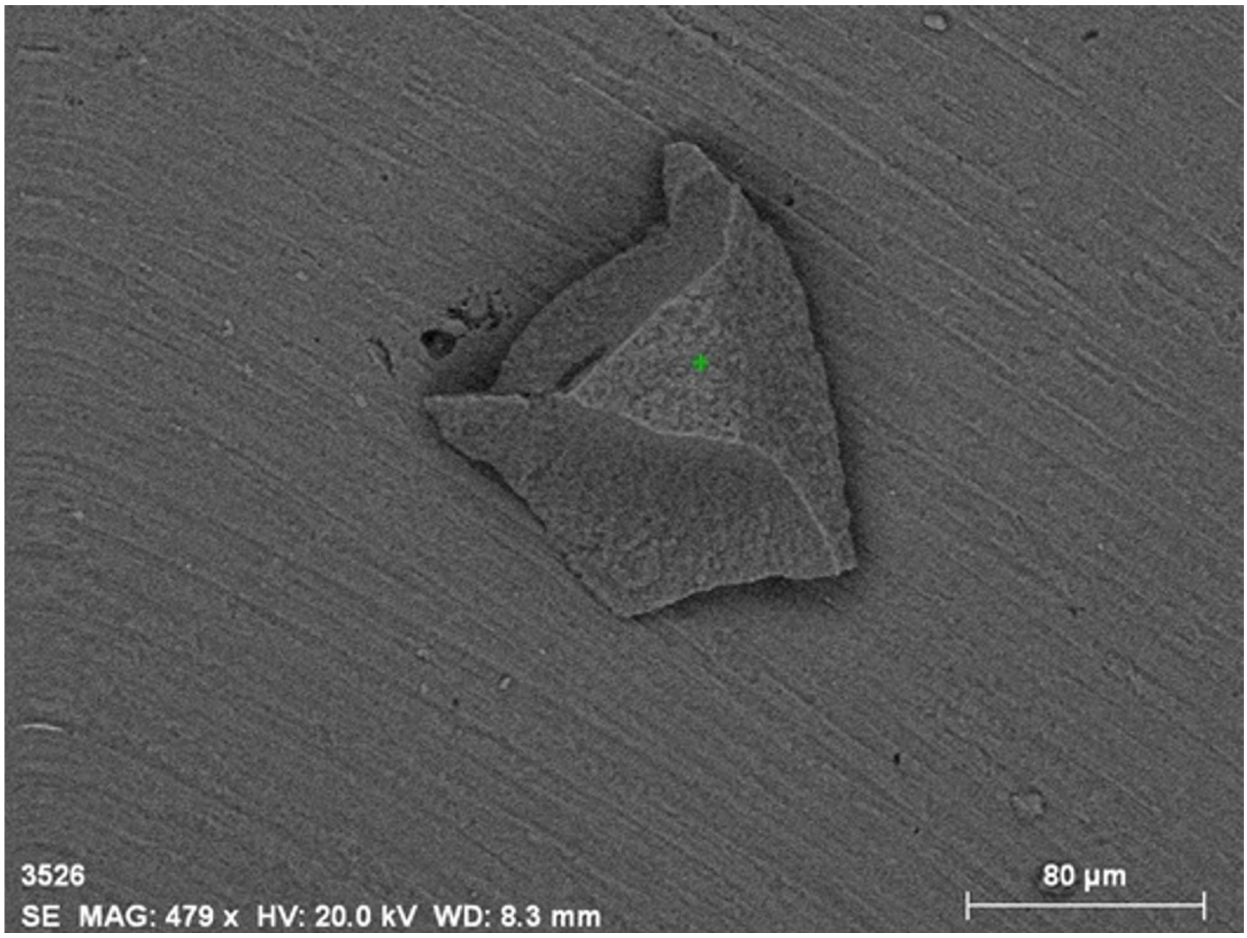

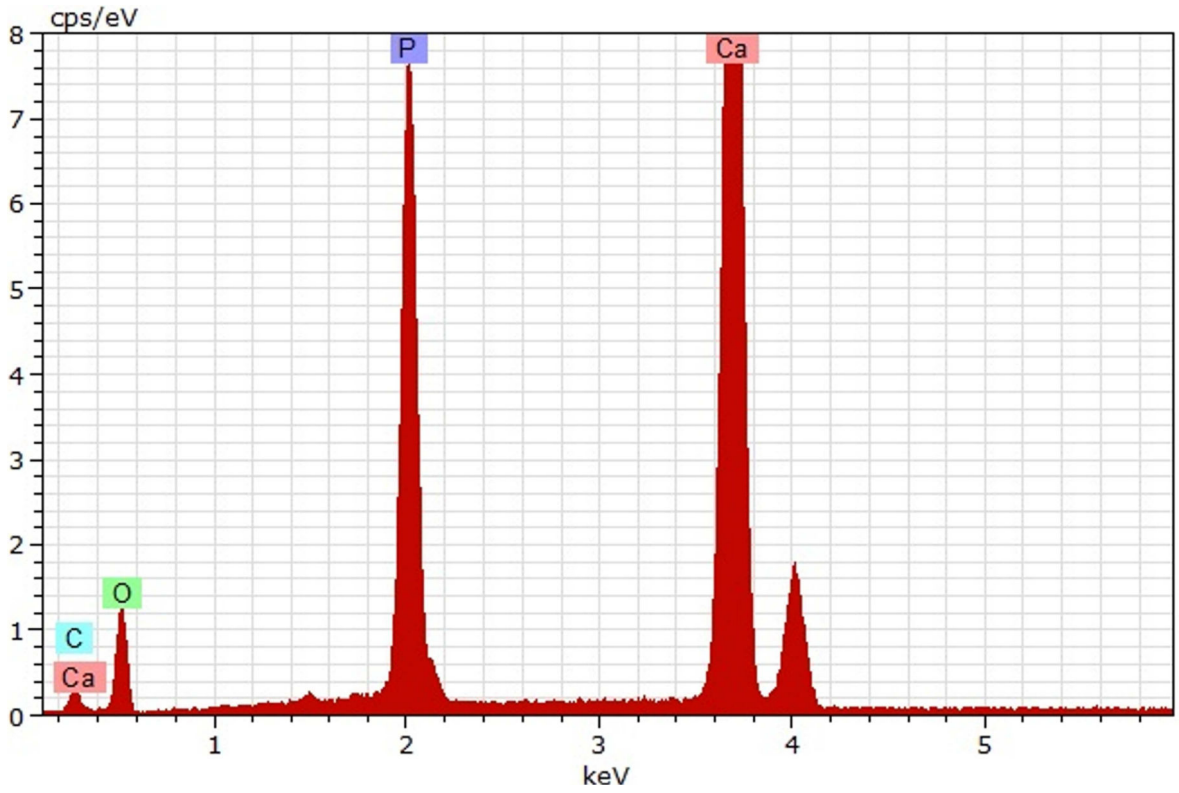

Figure 7.

A. SEM-EDS analysis. Intact surface of HA disc.

Figure 7B. SEM-EDS analysis. Elemental composition of point marked by pointer (green cross in center)

Figure 7C. SEM-EDS analysis. Pseudomonal acclivity alteration of HA disc.

Figure 7D. SEM-EDS analysis. Elemental composition of pseudomonal acclivity resembles that of intact HA structure. [Calcium (**Ca**), Carbon (**C**), Oxygen (**O**), Phosphorus (**P**)]

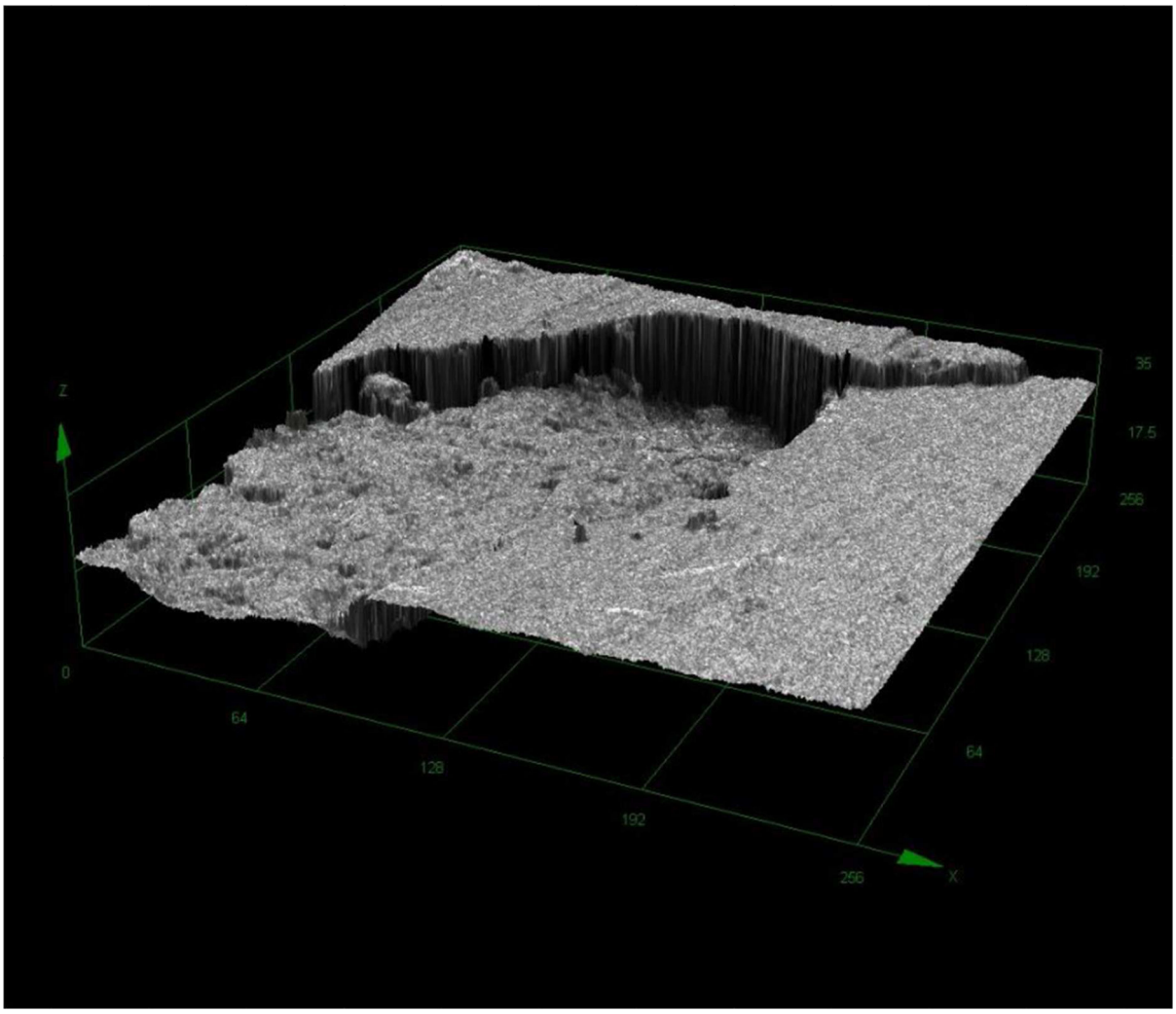

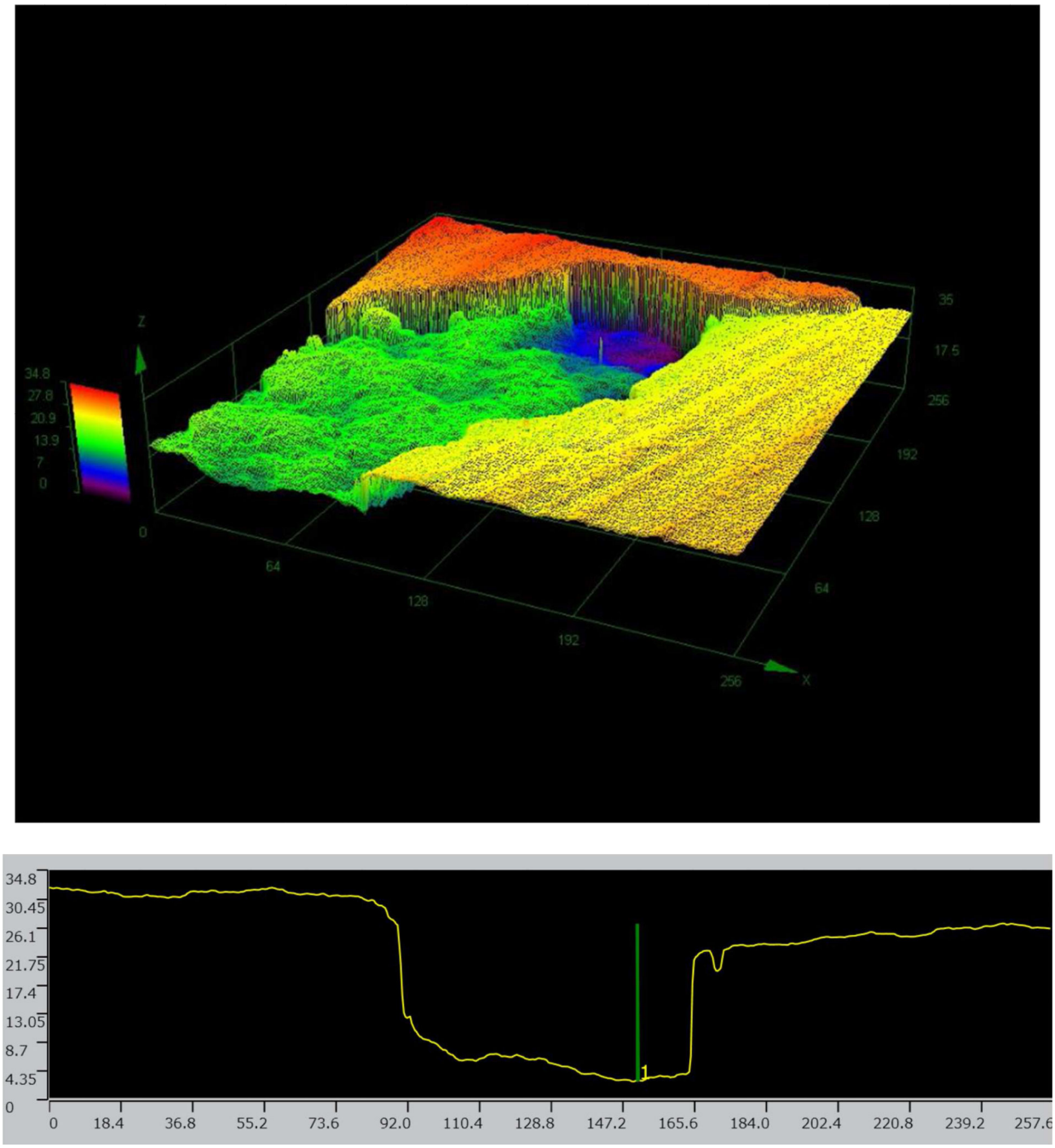

Figure 8.

Computerized planimetry assessment. **Top:** Confocal image [**1**] of a pseudomonal biofilm-induced cavity in HA surface.

Figure 8. Computerized planimetry assessment. **Top:** Confocal image [**2**] of a pseudomonal biofilm-induced cavity in HA surface.

Figure 8. Computerized planimetry assessment **Bottom:** Chart showing cavity's height/depth (OY) and width (OX) [μm^2].

Table 1

Conditions of biofilm growth.

Strain(s)	medium	time of incubation in the presence of HA discs	aerobic/anaerobic conditions
P.aeruginosa	TSB	72h	aerobic
S.aureus	TSB	72h	aerobic
S.mutans	BHIM+3%S	72h	facultatively anaerobic
S.mutans	BHIM	72h	facultatively anaerobic
C.albicans	TSB	72h	aerobic
Str.mutans + *C.albicans*	BHIM	72h	facultatively anaerobic

TSB – Tryptic Soy Broth; BHIM – Brain-Heart Infusion Medium; +3%S – medium supplemented with 3% sucrose.

Table 2

Cfu/mm^2/HA surface of the investigated strains.

Biofilm	medium	mean cfu × 10^3/mm^2	standard error of the mean
S.mutans	BHIM	7.5	0.35
S.mutans *	BHIM+3%S*	10.16*	0.97*
S. mutans from *C.albicans/S.mutans* mixed biofilm	BHIM	8.4	0.9
C.albicans from *C.albicans/S.mutans* mixed biofilm	BHIM	6.23	1.1
C.albicans	TSB	4.2	0.5
S.aureus	TSB	8.16	0.8
P.aeruginosa	TSB	6.9	0.65

BHIM – Brain-Heart Infusion Medium, BHIM+3%S - Brain-Heart Infusion Medium supplemented with 3% sucrose; TSB – Tryptic Soy Broth.

* when supplemented with sucrose, *S.mutans* forms mutan-containing extracellular matrix, which due to its durability, does not allow us to make precise estimations of cfu number. Thus, for this setting, cfu given is more of an indicative value. To omit this obstacle, assessments in BHIM without sucrose were also performed.

Table 3

Morphologic subtypes and characteristics of alterations observed on HA surfaces.

Type of alteration	Abbreviation	Lesion description	Produced by	Approximate surface area [μm^2]	Example
cavities	**[C]**	depression of irregular shape and diverse depth	all investigated strains in both biofilm and supernatant samples; found also in negative controls	$\pm 20 \mu m^2$ - $6000 \mu m^2$	Figure 3C,3D-3
pits	**[P]**	circular to ovoid deep depressions of distinctly smaller surface area as compared to cavities	*S.mutans* cultured in medium supplemented with sucrose; *S.mutans* in mixed biofilm	$\pm 20 \mu m^2$-$80 \pm 20 \mu m^2$	Figure 3D-1
deep recesses	**[L]**	depression of shape, depth and size similar to cavities; characteristic feature of recess is landslide-like regions partially covered by loosely adherent HA	all investigated strains in both biofilm and supernatant samples	$\pm 20 \mu m^2$ - $6000 \mu m^2$	Figure 3D-3, 3G-1
vast depressions	**[VD]**	multiple shallow defects forming a vast field of depressions in the HA surface	all investigated strains in both biofilm and supernatant samples	Not calculable; the largest among observed depressions.	Figure 3E
spherules	**[B]**	shallow, circular depressions in the HA surface	*S.mutans*, *S.aureus*, *C.albicans* cultured in both type of media	$\pm 40 \mu m^2$ - $100 \mu m^2$	Figure 3F, 3G-2
acclivities	**[PS]**	shard-shaped elevations from HA surface	*P.aeruginosa* only, found both in supernatant and biofilm samples	up to $\pm 120030 \mu m^2$; the largest among all observed alterations	Figure 3H

Table 4

Mean number of alterations observed in A: biofilm and **B**: cell-free supernatant samples.

A: biofilm samples	**Mean number of alterations**								
Types of alterations	**NC1**	**NC2**	**NC3**	***S.mutans* BHIM**	***S.mutans* BHIM+3%**	***C. albicans***	***P. eruginosa***	***S. aureus***	***C.albicans+Str.mutans***
Cavities	40.5±8.68	48.83±12.25	89.5±27.61	135.833±29.38	428.5±75.95	201.5±52.75	160.66±42.44	172±44.14	298±127
Pits	0	0	0	0	42.5±15.28	0	0	0	15.5±9
Deep Recesses	0	0	0	31±14.31	6±3.05	64.5±24.5	50.16±19.21	27.66±15.31	288.83±52.55
Vast Depressions	0	0	0	3.16±1.95	13.5±5.5	7.16±3.48	0	6±3.52	0
Spherules	0	0	0	15.33±13.31	0	10±7.23	0	6.33±3.93	0
Acclivities	0	0	0	0	0	0	142.16±61.37	0	0

B: cell-free supernatant	**Mean number of alterations**					
Types of alterations	***S.mutans* BHIM**	***S.mutans* BHIM+3%**	***C.albicans***	***P.aeruginosa***	***S.aureus***	***C. albicans+Str. mutans***
Cavities	78.83±13.33	179.16±44.95	206.83±73.19	178.16±	139.33±81.12	200.83±42.57
Pits	0	8±5.01	0	0	0	6.66±5.85
Deep Recesses	37.66±20.56	180.16±78.38	50±22.943	98.66±81.98	138.33±157.29	327.33±93.64
Vast Depressions	10±3.46	4.33±2.49	7±2.82	0	10.16±6.7	4,83±3.31
Spherules	23.33±	0	12±8.64	0	15.83±4.49	0
Acclivities	0	0	0	177.33±49.36	0	0

± standard deviation of mean. BHIM – brain-heart infusion media; +3%S – BHIM supplemented with 3% sucrose; NC1,2,3 – negative controls

Table 5

Observed pH changes over time for various strains.

		Time of incubation								
Strain	**pH of sterile medium**	**24h**			**48h**			**72h**		
		repeats n=3			**repeats n=3**			**repeats n=3**		
P.aeruginosa ATCC/TSB	7.4	8	8	8	8.5	8.5	8.5	8.5	8.5	8
S.aureus/TSB	7.4	6	6	6	6.5	6.5	7	7.5	7	7
C.albicans/TSB	7.4	6	6.5	6	8	8	8	5	5	5
***S.mutans*/BHI+3%S**	7.3	5	5	5	5	4.5	4.5	5	4.5	4.5
***S.mutans*/ BHIM**	7.1	6	6	5	5	5	5	5	5	5
S.mutans* + *C.albicans/BHIM	7.1	5	5.5	5	4.5	5	4.5	4.5	4.5	4.5

TSB – tryptic soy broth; BHIM – Brain-Heart Infusion Medium; +3%S – medium supplemented with 3% sucrose.